Design of Robust Active Trailer Steering Controllers for Multi-Trailer Articulated Heavy Vehicles Using Software/Hardware-in-the-Loop Real-Time Simulations

By
Mutaz Keldani

A thesis submitted to the
School of Graduate and Postdoctoral Studies in partial
fulfillment of the requirements for the degree of

Master of Applied Science in Automotive Engineering

Faculty of Engineering and Applied Science
University of Ontario Institute of Technology
Oshawa, Ontario, Canada

August, 2019

THESIS EXAMINATION INFORMATION

Submitted by: **Mutaz Keldani**

Master of Applied Science in **Automotive Engineering**

Thesis title: Design of Robust Active Trailer Steering Controllers for Multi-Trailer Articulated Heavy Vehicles Using Software/Hardware-in-the-Loop Real-Time Simulations

An oral defense of this thesis took place on July 17th, 2019 in front of the following examining committee:

Examining Committee:

Chair of Examining Committee	Dr. Martin Agelin-Chaab
Research Supervisor	Dr. Yuping He
Examining Committee Member	Dr. Xianke Lin
Thesis Examiner	Dr. Jing Ren, FEAS

The above committee determined that the thesis is acceptable in form and content and that a satisfactory knowledge of the field covered by the thesis was demonstrated by the candidate during an oral examination. A signed copy of the Certificate of Approval is available from the School of Graduate and Postdoctoral Studies.

ABSTRACT

Due to their remarkable economic and environmental benefits, Multi-Trailer Articulated Heavy Vehicles (MTAHVs) have been frequently adopted by the trucking industry. Despite the above advantages, MTAHVs exhibit two particular challenges concerning road safety. MTAHVs exhibit poor maneuverability at low speeds and low lateral stability at high speeds. To address these issues, an Active Trailer Steering (ATS) system using two control techniques is proposed. In recent years, the Linear Quadratic Regular (LQR) technique has been applied to the design of controllers for ATS systems of Articulated Heavy Vehicles (AHVs). In the LQR-based controller designs, all vehicle system parameters, e.g., forward speed and operating conditions, are assumed to be predefined. However, in real-life applications, the operating conditions, such as trailer payload and forward speed, may vary. Thus, the robustness of the LQR-based ATS controllers is doubted. To address this dilemma, a robust ATS controller is designed using the combined method of a Linear Matrix Inequality (LMI) and the LQR technique. To assess the robustness of the LMI+LQR-based ATS controller, the payload of the trailer and the dynamic parameters of the trailer steering actuator are introduced as the vehicle system parametric uncertainties. The performance of the proposed ATS controllers is evaluated using Software/Hardware-In-the-Loop (SHIL) real-time (RT) simulations. The results of the research indicate that the LMI+LQR-based ATS controller can achieve desired system performance under parametric uncertainties.

Keywords: B-train double, active trailer steering, LMI+LQR-based controller, trailer steering actuator, trailer payload, robust controller

† To my Teta, Om Hanna. †

AUTHORS DECLARATION

I hereby declare that this thesis consists of original work of which I have authored. This is a true copy of the thesis, including any required final revisions, as accepted by my examiners.

I authorize the University of Ontario Institute of Technology to lend this thesis to other institutions or individuals for the purpose of scholarly research. I further authorize University of Ontario Institute of Technology to reproduce this thesis by photocopying or by other means, in total or in part, at the request of other institutions or individuals for the purpose of scholarly research. I understand that my thesis will be made electronically available to the public.

_____

Mutaz Keldani

Statement of Contributions

I hereby certify that I am the sole author of this thesis and that no part of this thesis has been published or submitted for publication. I have used standard referencing practices to acknowledge ideas, research techniques, or other materials that belong to others. Furthermore, I hereby certify that I am the sole source of the creative works and/or inventive knowledge described in this thesis.

ACKNOWLEDGEMENTS

† "I can do everything through Him who gives me strength" †

Philippians 4:13

I would like to thank my thesis advisor, Dr.Yuping He, for his guidance throughout this project.

My sincere appreciation goes out to my beloved parents, George and Randa; my brothers and sister in law - Zaid, Said and Marlin - for their constant motivation and support throughout this journey. A special thank you to my mother for her unconditional support and the sleepless nights that she had to put up with.

I would also like to thank Priay Shastry for being by my side throughout this journey, thank you for making the long hard sleepless nights fun and productive, without you this journey would have been a bigger challenge.

I would also like to thank my second family - Hammad, Smitha, Saurabh, Tushita, Abhilash, Khizar, Heta, Navid, Rami and Romario - for being my support system throughout this journey. I would like to thank my brother from another mother, Qais, for always being my best supporter.

Last but not least, thank you to my cars - Hummer, BMW and Mini Cooper - for putting a smile on my face every day before going to school.

Contents

List of Figures

List of Tables

Abbreviations

MTAHV	Multi-Trailer Articulated Heavy Vehicle
ATS	Active Trailer Steering
LCV	Long Combination Vehicle
DOF	Degree Of Freedom
CG	Center of Gravity
ATDB	Active Trailer Differential Braking
ARC	Active Roll Control
RWA	Rearward Amplification
AHV	Articulated Heavy Vehicle
PFOT	Path-Following Off-Tracking
SAE	Society of Automotive Engineers
HIL	Hardware-In-the-Loop
LQR	Linear Quadratic Regulator
LMI	Linear Matrix Inequality
RT	Real-Time
MRAC	Model Reference Adaptive Control
VMT	Vehicle Miles Travelled
PID	Proportional Integral Derivative
SLC	Single Lane Change

UOIT	University of Ontario Institute of Technology
KF	Kalman Filter
DEKF	Dual Extended Kalman Filter
QPSO	Quantum Particle Swarm Optimization
MTO	Ontario Ministry of Transportation
EOM	Equation of Motion
LQG	Linear Quadratic Gaussian
FLC	Fuzzy Logic Control
SHIL	Software/Hardware-In-the-Loop
ATC	Actuator Time Constant
DHIL	Driver-Hardware-In-the-Loop

Chapter 1

Introduction

1.1 Multi-Trailer Articulated Heavy Vehicles

Long Combination Vehicles (LCVs) are widely used in numerous countries, such as USA, Sweden, Canada, and Australia. LCVs have been on Canadian roads for many years. For example, LCVs have been adopted in Quebec and Alberta since 1986 and 1969, respectively [1]. Moreover, the Ontario Ministry of Transportation (MTO) launched its LCV program in 2009 to ensure smooth LCV transportation between Ontario and Quebec [2, 3]. It is worth mentioning that LCVs are defined as road vehicles exceeding the length and weight of a typical tractor-semi-trailer, which is a commonly used single-trailer Articulated Heavy Vehicle (AHV) with a tractor and a semi-trailer [4]. MTAHVs are categorized into A-, B-, and C-trains based on the type of coupling mechanism used to connect the vehicle units. A coupling mechanism imposes a significant impact on the path-following off-tracking (PFOT) and lateral stability of the combination [1, 5]. The vehicle combination to be investigated in this thesis is a B-Train Double. The B-Train Double is composed of a tractor and two

semi-trailers. The first trailer is directly equipped with a built-in fifth wheel to connect the second trailer [2, 6].

There exist the following advantages associated with the use of MTAHVs [4]: 1) increase in the cargo space by 25% to 100% compared to that of the single-trailer AHV, 2) reduction in the number of tractors used on roads to transport the same amount of goods, and 3) reduction in the transportation costs due to fewer drivers and remarkable fuel consumption. Moreover, compared with single-trailer AHV, MTAHVs reduce fuel consumption and greenhouse gas emission by about 32% and decrease the tire-road wear by 40% [7, 8].

1.2 Motivations and Objectives

Despite the benefits associated with MTAHVs, these large vehicles exhibit poor low-speed maneuverability and low high-speed lateral stability due to multi-unit vehicle structures, heavy payloads, high Centers of Gravity (CGs), and long and high dimensions [2, 7–9]. Moreover, the majority of North America highway ramps and interchanges were designed in the early1950s without considering the geometries of MTAHVs [7, 10]. The highway ramps, where sudden vehicle speeds and steering changes occur, are susceptible to witnessing severe crashes [11].

From the design viewpoint, there exists a trade-off between the performance measures of MTAHVs at high and low speeds. At low speeds, MTAHVs experience poor PFOT; whereas, at high speeds, they exhibit low lateral stability, leading to three unstable motion modes, namely, trailer sway, jack-knifing, and rollover [5, 7, 12].

MTAHVs show remarkable benefits when compared to the single-trailer AHV. However, the length of the combination and the height of the CG frequently raise various concerns about the safety performance of MTAHVs. A study done in the USA, based on the fatal involvement rates according to the Vehicle Miles Travelled (VMT) among 13 states, shows a 2.88 per 100 million VMT involvement for single-trailer AHV and 3.13 per million VMT for MTAHVs. [4]. Another study shows that MTAHVs are likely to be involved in 11% more collisions per mile compared to single-trailer AHVs [1].

To address the above issues and improve the lateral instabilities of MTAHVs, the B-Train Double and an Active Trailer Steering (ATS) system are proposed in this thesis. Two controllers are implemented and validated using numerical simulations and Hardware-in-the-loop (HIL) Real-Time (RT) simulations. To evaluate the performance of the proposed controllers, the Rearward Amplification (RWA) performance measure is used. The RWA is discussed in details in Section 1.3.

Inspired by the above motivations, the objectives of this thesis can be established:

1) Derive and validate a linear four Degrees of Freedom (DOF) yaw-plane model, which is employed for the design and implementation of the ATS controllers.

2) Design and implement two controllers using the techniques of Linear Quadratic Regulator (LQR) and Linear Matrix Inequality (LMI).

3) Evaluate the designed controllers in terms of the RWA performance measure under a Single Lane Change (SLC) maneuver.

4) Evaluate the robustness of the proposed controllers under system parametric uncertainties, while ensuring the RWA ratio close to the value of 1.0.

5) Validate the performance of the robust controller using HIL-RT simulations.

1.3 Performance Measures

Compared with single-trailer AHVs, MTAHVs demonstrate remarkable benefits in many aspects. However, the unique instabilities at high speeds is a subject of significant debate over the last four decades [13]. To evaluate the safety performance of MTAHVs and active safety systems, a safety measure known as Rearward Amplification (RWA) ratio was proposed by Ervin and Guy in 1986. They defined the RWA as a measure to assess the lateral stability of MTAHVs under a SLC maneuver [14]. It was reported that the steering input frequency directly influences the RWA ratio [6]. Moreover, it was suggested that a steering frequency of 0.4 Hz excites the RWA of the MTAHVs [6, 15]. Numerically, the RWA ratio is defined as the peak lateral acceleration of at the rearmost trailer CG to the peak lateral acceleration at the Tractor CG under a SLC maneuver [14]. The RWA can be written as,

$$RWA = \frac{|ay_{RearmostTrailer}|}{|ay_{LeadingUnit}|} \tag{1.1}$$

where $ay_{RearmostTrailer}$ is the absolute value of the peak lateral acceleration at the rearmost trailer CG, and $ay_{LeadingUnit}$ is the absolute value of the peak lateral acceleration at the leading vehicle unit CG [6].

It was also reported that the RWA ratio increases when the combination undergoes sudden maneuver while travelling at high speeds (above 80 km/h) [4].

Moreover, it was shown that a low RWA ratio reduces the tendency of rollover for MTAHVs. It is concluded that the ideal value of the RWA ratio is 1.0 [12].

1.4 Methodology

To achieve the objectives introduced in Section 1.2, several steps are taken to ensure a smooth and rigid design process of an ATS system:

1) A 4-DOF yaw-plane model is derived and validated with a nonlinear yaw-roll model developed in the commercial software package, namely, TruckSim. An open-loop SLC maneuver is then simulated within the TruckSim-MATLAB/Simulink co-simulation environment. After that, the responses of both the linear and nonlinear models are compared to justify whether the 4-DOF model is a good fit for the design and implementation of ATS system controllers.

2) The LMI and LQR techniques are combined and implemented to improve the lateral stability of the B-Train Double. The RWA measure is used to assess the performance of the proposed controllers.

3) The LQR-based and the LMI+LQR-based controllers are examined, and their robustness is validated by exposing the controllers to parametric uncertainties, e.g., trailers' payload and steering Actuator Time Constant (ATC).

4) The robust controller out of the two controllers is then validated using HIL-RT simulations, where a physical axle is connected to a vehicle driving simulator to simulate the SLC maneuver.

1.5 Thesis Contributions

In this thesis, the performance of B-Train Double under system parametric uncertainties was examined. The lateral stability of the B-Train Double was evaluated under over 20 different operating conditions. The results are then analyzed and compiled in the form of a database, to help future researchers understand the behaviour of B-Train Doubles under the exposure of uncertain parameters. The main contributions are summarized as follows:

- Design of an optimal controller known as the LQR-based controller for the ATS system to improve the lateral stability of the combination while maintaining the RWA ratio close to the value of 1.0. The proposed controller is implemented using a hand derived 4-DOF yaw-plane model.
- Due to robustness concerns associated with the LQR-based controller under the exposure of system uncertainties, a robust control technique is proposed. To the knowledge of the author, to date, the LMI+LQR-based controller has not been employed to the ATS system for B-Train Double.
- Numerical and HIL-RT simulations were performed in the presence of system parametric uncertainties. Moreover, the impact of the actuator dynamic parameters is evaluated, which is another critical feature that has not been applied to ATS systems for B-Train Doubles.

1.6 Thesis Organization

The remainder of the thesis is organized as follows. Chapter 2 provides an overview of the previous studies done on passive and active safety systems to

enhance the lateral stability of MTAHVs at high speeds and to improve the maneuverability of MTAHVs at low speeds. Chapter 3 presents the key elements required to design the ATS system. A linear model is derived, validated and employed to design the ATS controller. Also, a brief overview of the two types of controllers is discussed. Chapter 4 offers an extensive study on the response of the B-train model to a predefined SLC maneuver input. The B-Train Double is evaluated based on three modes: passive, LQR-based controller, and LMI+LQR-based controller. Finally, Chapter 5 presents the conclusions derived from this research and provides recommendations for future studies.

Chapter 2

Literature Review

2.1 Introduction

This chapter introduces the various configurations of MTAHVs and the typical linear vehicle models used to design and develop active safety systems for these vehicles. In addition, it provides an overview of past achievements related to ATS systems. Moreover, control techniques used in the implementation of several ATS systems are reviewed.

2.2 MTAHVs models

LCVs have been used across Canada and the United States of America for decades [16, 17]. In 2009, Ontario launched their LCV program [2], after an extensive study by Francher and Winkler on the configurations and performance measures of AHVs [6, 12]. As stated earlier, MTAHVs are categorized into three different classes depending on the types of mechanical couplings between the

vehicle units [2, 5–9, 12, 14, 18]. The three types are known as A-, B-, and C-Trains. In this research, a B-Train Double combination is used to implement an ATS system.

Due to the complexity of the B-Train Double configuration, numerous studies [3, 5–9, 15, 18–27] have proposed various linear models to simplify the design of the ATS controllers. The linear models are generally classified into yaw-plane models and yaw-roll models. In [5, 8], a 4-DOF yaw-plane model was used in the design and implementation of an ATS system, where the pitch and roll motions were neglected. In [25], a 7-DOF yaw-roll model was proposed to investigate the effect of roll dynamics on the lateral stability of MTAHVs. The previous studies [5, 8] indicate that the 4-DOF yaw-plane model used in this work has been validated with a nonlinear TruckSim model. The results of the lateral dynamics demonstrate good agreement between the linear and nonlinear models under specified circumstances, e.g., the absence of aerodynamics, constant forward speed, roll and pitch angles are neglected, and small steering input to the combination is assumed to guarantee linearity of the system.

Islam et al. [25] carried out a study to investigate the dynamics of a B-Train Double represented by a 4-DOF yaw-plane model and a 7-DOF yaw-roll model. At first, they validated both models using a nonlinear TruckSim model. The simulation results for the validation showed that both models preserved the dynamics characteristics despite a slight variation in the lateral acceleration curves. In addition, the authors noted that the main reason behind the slight deviation is due to the lack of load transfer capabilities in both the linear models. Lastly, the authors suggested that both the linear models are justified to be used for linear controller designs under low-g maneuvers.

The following section reviews the various ATS controllers designed using the 4-DOF yaw-plane models.

2.3 Safety Systems

2.3.1 Passive Safety Systems

To understand the ATS systems proposed in the literature, it is essential to grasp the main issues in a conventional multi-unit combination. Past simulation and testing results demonstrated that the MTAHVs exhibit poor maneuverability at low speeds and low lateral stability at high speeds due to their multi-unit configurations, large sizes and high CGs [5, 7, 23, 25, 26, 28, 29].In addition, conventional MTAHVs use solid non-steerable axles, which result in excessive scrubbing between the tires and road surfaces during sharp turns, undesired cut-in of the rearmost trailer and yaw instabilities [30, 31].

In [31–33], several passive steering systems were proposed to solve the tire-road scrubbing issue and improve the low-speed maneuverability. It was also indicated that these passive mechanisms steer some of the trailers wheels based on the geometrical correlation. However, Prem and Atley argued that such passive systems result in significant path-tracking errors in transient maneuvers [34]. In addition, it was reported that passive steering systems influence the lateral stability of the combination, resulting in higher lateral acceleration.

In 2002, Jujnovich and Cebon carried out a study on semi-trailers self-steering axles [35]. The study shows that the self-steering system has a positive impact on the low-speed performance of semi-trailers. The examined system reduces the vehicles swept path width, lateral tire forces, tire scrubbing and wear, and

lastly increases the maneuverability of the combination. However, it is also noted that the gained advantages are achieved at the expense of poor performance at higher speeds, i.e., increased RWA ratio and yaw-instabilities.

It can be concluded from the past studies that passive systems have limitations and result in poor high speed lateral stability [7, 35]. The various operating conditions, e.g., trailer payload and road curvature, limit the use of these passive systems [12]. The limitations behind passive systems are the motivations for studying active safety systems, e.g., ATS [5, 8, 21], Active Trailer Differential Braking (ATDB) [36–39], Active Roll Control (ARC) [40–45] and some integrated systems combining multiple active systems [46].

2.3.2 Active Safety Systems

The main objectives of the proposed active safety systems are to increase the lateral stability at high speeds and improve the path following at low speeds, thereby mitigating tire-road scrubbing and preventing yaw instabilities. It was well established in the literature that ATS systems can achieve both objectives without reducing the forward speed of the combination [7, 47] which is one of the drawbacks of ATDB [47, 48]. In this thesis, an ATS system is proposed to achieve the stated objectives.

In 2011, Cheng et al. [30] a high-speed optimal ATS for tractor-semi-trailer was proposed. A linear 5-DOF yaw-roll model was derived and employed for the controller design. The proposed ATS scheme consists of two controllers to minimize the path-tracking error in steady- state maneuver while improving the roll stability under transient maneuvers. The researchers developed a method to switch between two control modes based on the severity of the maneuver.

It was indicated that the ATS scheme improved the high-speed PFOT by 57% under a lane change maneuver while reducing the trailers lateral acceleration by approximately 27%.

In Kharrazi et al. [47], the lateral stability of several combinations was investigated. Based on the simulation results, it was shown that passive safety systems lack lateral stability and require an external active system to improve their dynamics. Thus, the investigators proposed an ATS system using a generic controller to improve lateral stability. The proposed system reduces the offtracking and trailing sway without degrading the maneuverability of the combinations.

In 2007, Rangavajhula and Tsao proposed an ATS system using several control schemes to reduce the offtracking of an AHV using the RWA as a performance measure [49]. The investigators developed a 5-DOF yaw-plane model for the controller design and implementation. The examined combination consists of a leading unit and three trailing units. The main objectives were to reduce the RWA ratio while gaining an accurate tractor-track following. Based on the simulation results, it was demonstrated that at least two of the three trailers should be equipped with an ATS system for the combination to minimize the RWA ratio and to reduce the offtracking. The investigators also examined the effect of a command steering system [50]. It was indicated that the command steering has a significant effect on the offtracking at low speeds, and reduces the turning radius under a 90 degree turn. It was also noted that the proposed ATS system had a moderate improvement on the RWA ratio at medium to high speeds.

In 2010, Odhams et al. proposed an ATS for AHVs [51]. The target vehicle in this study was a tractor-semi-trailer combination, where the fifth wheel on

the leading unit projects a path for the trailer to follow. The investigators concluded that the fifth wheel connecting the trailer to the leading unit introduces undesirable yaw instabilities at high speeds. It was noted that the combination exhibited high lateral acceleration under sudden maneuvers, resulting in higher RWA ratio. Additionally, at high speeds, the yaw damping ratio decreases, resulting in an overshoot in the trajectory of the rear unit. Based on the simulation results of an SLC test conducted in this study, the peak path error was reduced by approximately 33%, while reducing the RWA by about 35%. The gathered simulation and experimental results indicated that the proposed ATS system improved the low-speed maneuverability and high-speed stability, reduced tire wear, and reduced the severity of rollover threshold under high-speed transient maneuvers.

In a similar study on ATS for AHVs, Saeedi et al. proposed an integrated system combining ATS and ARC for a semi-trailer carrying liquid [52]. In this research, two vehicle models were developed and used for the implementation of the proposed systems. First, a 16-DOF nonlinear model was developed for the design of the ARC controller, and a 3-DOF linear model was derived for the design of the ATS controller. The achieved results showed that the proposed ATS improved lateral stability while improving maneuverability with the elimination of offtracking. It was noteworthy that combining both active systems improved not only the path tracking and maneuverability performance, but also had a positive impact on the rollover risk.

Other researchers examined the influence of ATS on the dynamics of a tractor-semi-trailer combination [53–55]. In these studies, various control schemes were developed utilizing linear and nonlinear models. Since the application

of ATS to AHVs demonstrated a positive influence on the maneuverability and lateral stability, researchers have proposed the use of these systems on more complex multi-trailer articulated heavy vehicles.

As stated before, MTAHVs show poor maneuverability at low speeds and low lateral stability at high speeds. He et al. [7] are one of the research investigators who investigated MTAHVs and introduced an ATS to improve the directional performance. The proposed ATS system operates in one of two modes depending on the forward speed of the vehicle. The first mode, namely PFOT, is activated when the combination is travelling at a speed less than 60 km/h; the second mode, called RWA, functions at speeds higher than 60 km/h. Since each mode operates within different speed ranges, the two controllers were designed and executed independently. The ATS simulation results show an enhancement in the maneuverability and lateral stability of the B-Train Double combination. In a similar study, Odhams et al. proposed an ATS system that has a forward and reverse operating modes [17]. The forward mode is achieved through steering five trailer axles, while the reverse mode is implemented using an on-board joystick and a vision system to assist the driver. It was shown that the proposed ATS improved offtracking in the forward direction, and completed a teardrop maneuver in the reverse direction.

The trade-off between the maneuverability and lateral stability of MTAHVs continues to be an active research area. Numerous researchers [5, 8, 9, 19, 21, 56] proposed various control methods to achieve a feasible design that would increase the number of MTAHVs on the roads.

2.4 Control Techniques

To design a functional ATS system, two main components are required: the hardware needed to actuate the steering of trailer wheels, and the software for calculating control commands considering the dynamic states of the vehicle. Several control techniques have been studied and utilized to design ATS systems, e.g., LQR [30, 49, 50, 54, 54, 57, 58], Linear Quadratic Gaussian (LQG) [5, 59], LQR+LMI [21, 24], Slide Mode Control (SMC) [52], Model Reference Adaptive Control (MRAC) [58], Fuzzy Logic Control (FLC) [60], μ-synthesis [5, 59], H∞ [8, 61, 62] etc.

In 2007, Rangavajhula and Tsao developed an ATS controller for a MTAHV, which consists of a tractor and three full trailers [49]. The ATS controller aimed at minimizing the PFOT by reducing the RWA ratio of the combination. The controller was designed using the LQR technique. The investigators used the same control method in 2008 to design a command steering for the same complex combination [50]. The robustness of the LQR-based controller was examined with the variation of tire parameters. The simulation results indicated that the LQR-based controller is notably robust to tire parameter variations. The similar LQR-based controller was also investigated by El-Gindy et al. [63]. The proposed control method accomplished the goal of improving the PFOT and enhancing the lateral stability [49, 50].

The LQR technique is an optimal control scheme that could be utilized in different systems and applications. In 2011, Cheng et al. introduced a high-speed ATS system for a tractor-semi-trailer using the LQR technique [30]. In this study, two controllers were designed, one to enhance the path following and

the other to improve the roll stability of the combination at higher speeds. A switching mechanism was designed to switch the operation between both controllers to guarantee an efficient and effective system. The robustness of the proposed control scheme was examined under various road surface conditions, sudden crosswind and road camber. The simulation results demonstrated the robustness of the proposed control scheme under the parametric uncertainties. Similarly, Warrier proposed an ATS for a tractor-semi-trailer combination [57]. The researcher concluded that the controller improved low-speed maneuverability and high-speed stability. The tuning of the LQR-based controller was not emphasized in [30, 57], and it was assumed that the trial and error method was used to determine the weighting factors in the design of the LQR-based controller.

Since tuning the LQR-based controller using the trial and error method could be time-consuming, in 2013, Islam and He proposed an optimization method to optimize both the weighting factors and passive vehicle design variables simultaneously [46]. Recently, Milani et al. used a similar method to tune the LQR-based controller using an optimization approach known as Quantum Particle Swarm Optimization (QPSO) [54]. Interpolation was employed to determine weighting factors for a range of given speeds. The QPSO approach simplifies the tuning process based on three different cases to ensure a wide operating range of the LQR-based controller. In the first case, maintaining an RWA ratio of unity was the objective of the controller. Results of case 1 showed accurate tracking of the combination while maintaining an RWA of unity. However, it was noted that roll stability was not improved compared to that of the baseline combination. The second case was implemented to maintain an RWA of less

than one. Simulation results indicated that this controller with such objective resulted in a significant improvement in the roll stability of the combination. Though it introduced a tracking error and increased steering input values. The last case combined two systems, which were an ATS and ARC systems. The simulation results showed the improvement of roll stability and PFOT. However, the investigators declared that the integrated controller would result in a highly complex hardware/software structure that consumes much energy. Kim et al. used a similar approach to optimize the LQR-based controller [55]. The main purpose of the ATS is to minimize the slip angle by following a reference yaw rate model.

The literature indicates that the LQR-based controllers may improve the maneuverability and lateral stability of AHVs. However, it should be noted that the LQR-based controller design requires measurements of all states for feedback control implementation [64]. Since some states are difficult to be measured, e.g., side slip angles, Cheng and Cebon proposed a method to estimate vehicle states, thereby enhancing the control implementation [65]. In this study, two state estimation methods were presented: 1) Kalman Filter (KF), and 2) Dual Extended Kalman Filter (DEKF). Both methods were analyzed and validated with a nonlinear TruckSim model. The simulation results showed reasonable accuracy considering the nature of the model. In addition, an experimental vehicle was used to verify the proposed estimation approaches and validate the simulation results.

In 2013, Jujnovich and Cebon proposed a path-following steering scheme for a tractor-semi-trailer combination [66]. This study evaluated a control method developed by Hata et al. in 1989 [67]. Jujnovich and Cebon also investigated

the method by Notsu et al. [68], where the same control method proposed by Hata was applied on an AHV to minimize the tail motion. Jujnovich and Cebon argued: 1) the control algorithm proposed by Hata by Hata and Notsu could only be used on simple systems operating at low speeds, 2) the proposed control method by Hata and Notsu did not consider typical operating conditions of AHVs, which have different requirements for the design of a controller, 3) no evidence was presented for high-speed testing. In [66], a controller with a low-speed and a high-speed mode is proposed to solve the previous challenges. A low-speed mode was utilized where the rear of the trailer follows a trajectory path projected by the fifth wheel. This method was first proposed by Notsu [68]. The second mode was developed for high speeds, where a Proportional Integral Derivative (PID) controller was introduced to align the yaw rates of the real trailer with those of the reference model. The investigators then combined both control modes, and the resulting controller controls the vehicle dynamics at low and high speeds. Simulation results showed that the proposed controller resulted in an improvement in low-speed maneuverability and high-speed stability. A similar study was conducted by A M C Odhams et al. [51]. In this research, the same controller reported in [66] was tested on an experimental vehicle. The field test results showed good agreement with those of the simulations.

In 2017, Sikder proposed an ATS system for B-Train Double using three different control methods [5]: 1) LQR, 2) LQG, and 3) μ-synthesis. The LQR-based controller showed improved lateral stability and maneuverability when compared to the baseline model. However, the LQR-based controller had a drawback when measured noises were introduced to the system. To address such

issues, the investigator designed an LQG-based controller by adding a KF to the LQR-based controller. The LQG-based controller showed remarkable results compared to those of the LQR-based controller and the baseline design when external noises were introduced to the system. The investigator noted that when designing the LQR- and LQG-based controllers, all the parameters were known and remained constant. However, in reality, vehicle system parameters, e.g., vehicle forward speeds and payloads, vary. To address this issue, the μ-synthesis controller was proposed and tested. To examine the robustness of the μ-synthesis controller, the stability of the B-Train Double was tested under a random combination of 13 parametric uncertainties. The simulation results demonstrated that the μ-synthesis controller improved the lateral stability of the vehicle regardless of the exposure to noise and parametric uncertainties.

In a study carried out by Kharrazi et al., an ATS system was tested on nine different AHV combinations [47]. A generic controller was designed to improve the lateral stability of AHVs at high speeds. To achieve the objective, the RWA ratio was reduced without degrading the maneuverability. No evidence shows the robustness of the generic controller, and the robustness of the generic controller is questionable. In 2012, Kharrazi further investigated the robustness of the controller [48]. To test the robustness of the controller, the system was exposed to vehicle parameter uncertainties, e.g., mass, moment of inertia, CG location tire cornering stiffness, etc. All the vehicle uncertainties were tested on high and low friction surfaces to study the effect of such surfaces on the performance of the proposed controller. The simulation results indicated that the controller was considerably robust and continued to enhance the lateral stability while considering parametric uncertainties. It was also noted that the PFOT

improvement was not uniform compared with the RWA results. Lastly, it was observed that the controller was more sensitive to parametric uncertainties on low friction road surfaces.

Barbosa et al. proposed a robust path-following controller for AHVs [61]. To evaluate the robustness of the controller, the system was subjected to parametric uncertainties. The payload of the trailer was selected as a parametric uncertainty, where four different payloads were examined. Two different robust controllers, i.e., a robust LQR (RLQR) and a H∞, were proposed to investigate the influence of parametric uncertainties on the performance of the system [69]. The simulation results indicated that the RLQR was more robust compared to the H∞. In addition, compared with the H∞, the RLQR enhanced the lateral stability, while maintaining outstanding maneuverability. A similar study for examining the effect of different payloads was conducted by Wang et al. [58]. In this study, a model reference adaptive control (MRAC) technique was used to design a controller to improve the lateral stability of the combination. A LQR-based reference model was used to enhance the robustness of the MRAC controller. The MRAC controller succeeded in improving the RWA measures by mimicking the behaviour of the reference model as intended in the design process.

Another robust control technique, which demonstrates remarkable capabilities of handling parametric uncertainties, is known as the linear matrix inequality (LMI) method. Many researchers used the LMI method to improve the robustness of the LQR- and H∞-based controllers. The LMI+LQR-based control method was utilized previously in the design of an active front steering controller for a sport utility vehicle with the variation of tire cornering stiffness and

forward speed [70]. Other researchers used LMI+LQR-based control method in different applications due to its robustness and ease of implementation, where one control gain could potentially negotiate all ranges of system uncertainties. In 2016, M. Sever et al. proposed an active trailer differential braking (ATDB) system to enhance the yaw stability of car-trailers [71]. The ATDB system was designed using the same robust control technique. In this study, the variation of forward speed was used as a parametric uncertainty to examine the robustness of the proposed controller. The simulation results indicated that the controller improved the yaw-stability of the car-trailer combination for a wide range of speed.

Ni and He [24] proposed an ATS system for an A-Train Double. In this study, the concerns related to the robustness of the LQR-based controllers were discussed. The LQR-based controller is not considered to be robust since it is designed based on predefined parameters, and vehicle parameters are assumed to be constant. Thus, it is not uncommon to doubt the robustness of the control system in the presence of parametric uncertainties. To address the challenges faced in the LQR-based controllers, the investigators proposed a robust controller using the LMI+LQR technique. To examine the robustness of the LMI+LQR-based controller, vehicle and trailer steering axle actuation parametric uncertainties were introduced to the system. To further enhance the robustness of the controller, a genetic algorithm was used to optimize the weighting functions and minimize the objective functions of the LMI+LQR controller design. The LMI+LQR-based controller was designed considering the fact that a constant gain could be used for all uncertain parameters of a dynamic system. The investigators also designed an H∞-based controller as another robust

controller. The performance of the two controllers was tested and validated using software and HIL testing. The achieved results showed excellent agreement between numerical simulation results and real-time simulation results and hardware. It was concluded that both the LMI+LQR- and the H∞-based controllers improved the lateral stability of the combination under parametric uncertainties.

Numerous researchers [72–74] used HIL real-time simulation to validate the performance of their control systems. It is commonly accepted that compared with field and road tests, HIL real-time simulation shows the following advantages [72]: 1) cost-effective, 2) safe, 3) flexible, and 4) easy for implementation. An ATS system was proposed and validated using HIL real-time simulation [75].

2.5 Summary

This chapter first reviewed the configuration of MTAHVs and their unique dynamic characteristics. Also, the primary safety concerns were discussed, which include the poor low-speed maneuverability and low high-speed lateral stability. To improve the directional performance of the MTAHVs, researchers investigated various passive safety systems. It was found that these passive trailer steering systems can improve the maneuverability at low speeds. However, they degrade the lateral stability at high speeds. To address the limitations of the passive trailer steering systems, various ATS systems were proposed and designed to improve the high-speed lateral stability while maintaining good

low-speed maneuverability. Past studies indicate that ATS systems are excellent candidates to increase the safety of MTAHVs.

To achieve an effective and robust ATS system, many control techniques were studied. The LQR technique was extensively utilized for the design of optimal controllers due to the ease of design and simplicity of tuning. However, it was concluded that the LQR-based controllers failed to maintain the stability of MTAHVs under system parametric uncertainties. A control technique known as the LMI+LQR method was explored, and it was found that the combined technique demonstrated superior robust performance under parametric uncertainties.

Chapter 3

Design of Controllers for Active Trailer Steering Systems

3.1 Introduction

This chapter designs two controllers for active trailer steering (ATS) systems of a B-Train Double. To this end, a 4-DOF yaw-plane model is generated to represent the B-Train Double. A comparative study is conducted, with which the yaw-plane model is validated using a nonlinear model developed in TruckSim software package. The stability boundaries of the B-Train Double is then examined by performing an extensive sensitivity analysis, which is implemented using eigenvalue analysis method under the variation of trailers' payload. Built upon the eigenvalue analysis, two controllers, namely the LQR- and LMI+LQR-based, are designed for ATS systems of the B-Train Double. The robustness of the controllers is examined considering two parametric uncertainties, i.e., trailers' payload and steering ATC.

3.2 Vehicle System Modeling

Figure 3.1 shows the configuration of the B-Train Double, which consists of a tractor and two semi-trailers. As shown in the figure, adjacent vehicle units are connected by a fifth wheel. The tractor has a front steerable axle and two solid rear axles; each of the trailers has three solid axles. Additional information regarding the vehicle parameters is provided in Appendix A.

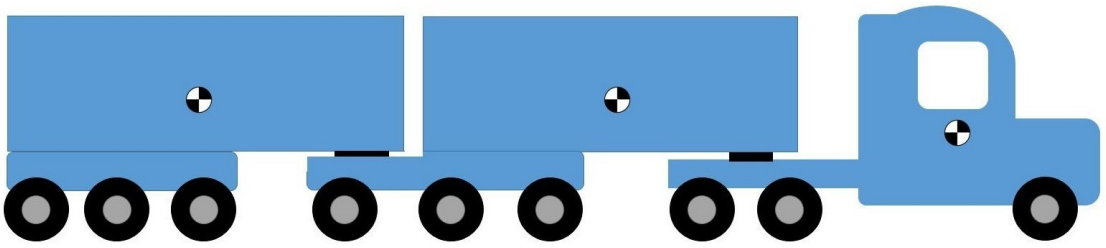

FIGURE 3.1: Schematic representation of the B-Train Double.

Figure 3.2 shows the 4-DOF yaw-plane model. In this model, a single wheel is used to represent each of the solid axles.

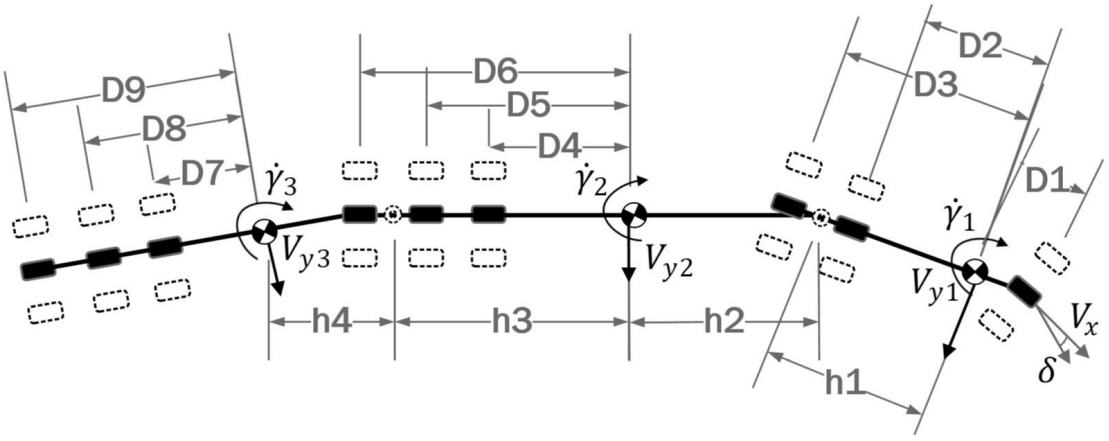

FIGURE 3.2: Schematic diagram, showing the degrees of freedom of the 4-DOF yaw-plane model.

In the yaw-plane model, four motions are considered: the lateral velocity of the tractor (V_{y1}), the yaw rate of the tractor ($\dot{\gamma}_1$), the yaw rate of the first trailer

($\dot{\gamma}_2$), and the yaw rate of the second trailer ($\dot{\gamma}_3$). Note that in Figure 3.2, subscripts 1, 2, and 3 are used to denote the tractor, the first trailer, and the second trailer, respectively. To derive the linear 4-DOF yaw-plane model, the following assumptions are made [5, 8]:

1) All units are moving at an equal forward speed ($V_x = V_{x1} = V_{x2} = V_{x3}$).

2) The units operate at a constant speed without the effect of any braking or aerodynamic forces.

3) The articulation angles between the units are small.

4) The pitch and roll motions are neglected.

5) The tire model used is linear.

The governing Equations of Motion (EOM) for the vehicle system are derived using the body-fixed coordinate system. Following the Newton-Euler approach, the EOMs of the tractor are,

$$m_1(\dot{V}_{y1} + V_x\dot{\gamma}_1) = F_{y1} + F_{y2} + F_{y3} - F_{h1} \tag{3.1}$$

$$I_1\ddot{\gamma}_1 = D_1F_{y1} - D_2F_{y2} - D_3F_{y3} + F_{h1}h_1 \tag{3.2}$$

the EOMs of the first trailer are,

$$m_2(\dot{V}_{y2} + V_x\dot{\gamma}_2) = F_{y4} + F_{y5} + F_{y6} - F_{h2} \tag{3.3}$$

$$I_2\ddot{\gamma}_2 = -D_4F_{y4} - D_5F_{y5} - D_6F_{y6} + F_{h1}h_2 + F_{h2}h_3 \tag{3.4}$$

and, the EOMs of the second trailer are,

$$m_3(\dot{V}_{y3} + V_x\dot{\gamma}_3) = F_{y7} + F_{y8} + F_{y9} + F_{h2} \tag{3.5}$$

$$I_3\ddot{\gamma}_3 = -1(D_7F_{y7} + D_8F_{y8} + D_9F_{y9}) + F_{h2}h_4 \tag{3.6}$$

The kinematic constraint equations for the first and second fifth wheels are expressed as,

$$\dot{V}_{y2} + \ddot{\gamma}_2 h_2 = \dot{V}_{y1} - \ddot{\gamma}_1 h_1 + V_x\dot{\gamma}_1 - V_{x2}\dot{\gamma}_2 \tag{3.7}$$

$$\dot{V}_{y3} + \ddot{\gamma}_3 h_4 = \dot{V}_{y2} - \ddot{\gamma}_2 h_3 + V_x\dot{\gamma}_2 - V_{x3}\dot{\gamma}_3 \tag{3.8}$$

The tire lateral forces are expressed as,

$$F_{yi} = -C_i * \alpha_i, \qquad i = 1, ..., 9 \tag{3.9}$$

where α and C are known as the tire slip angle tire cornering stiffness, respectively.

For the design of the LQR- and LMI+LQR-based ATS controllers, the above governing equations are expressed in the state space form as,

$$\dot{x(t)} = Ax(t) + C\delta(t) \tag{3.10}$$

$$x = [\, V_{y1} \quad \dot{\gamma}_1 \quad V_{y2} \quad \dot{\gamma}_2 \quad V_{y3} \quad \dot{\gamma}_3 \,]^T \tag{3.11}$$

where, A and C are the system and disturbance matrices, respectively.

TruckSim software package is used heavily throughout this research to validate the linear model and test the performance of the designed ATS systems. TruckSim is a multi-dynamics software package designed and validated based on experimental data [76]. Using such software package, researchers may test the performance of their controllers under severe scenarios at low cost while eliminating the safety concerns associated with field testing.

3.3 Model Validation

To validate the derived linear 4-DOF model, the open-loop maneuver specified in SAE J2179 is simulated [77]. In the test procedure, a co-simulation environment is established by connecting MATLAB/Simulink and TruckSim using an S-function. The linear 4-DOF model is derived in MATLAB, while the nonlinear B-Train Double model is developed in TruckSim. With the same steering input for the open-loop test maneuver, the resulting dynamic responses of the linear 4-DOF model and the TruckSim model can be directly compared and analyzed. The open-loop test procedure is a SLC maneuver. It is required that over the maneuver, the steering input is a single-cycle sinewave with a frequency of 0.4 Hz, and the testing vehicle travels at a constant forward speed of 88 km/h. Figure 3.3 shows the steering input recommended by SAE J2179.

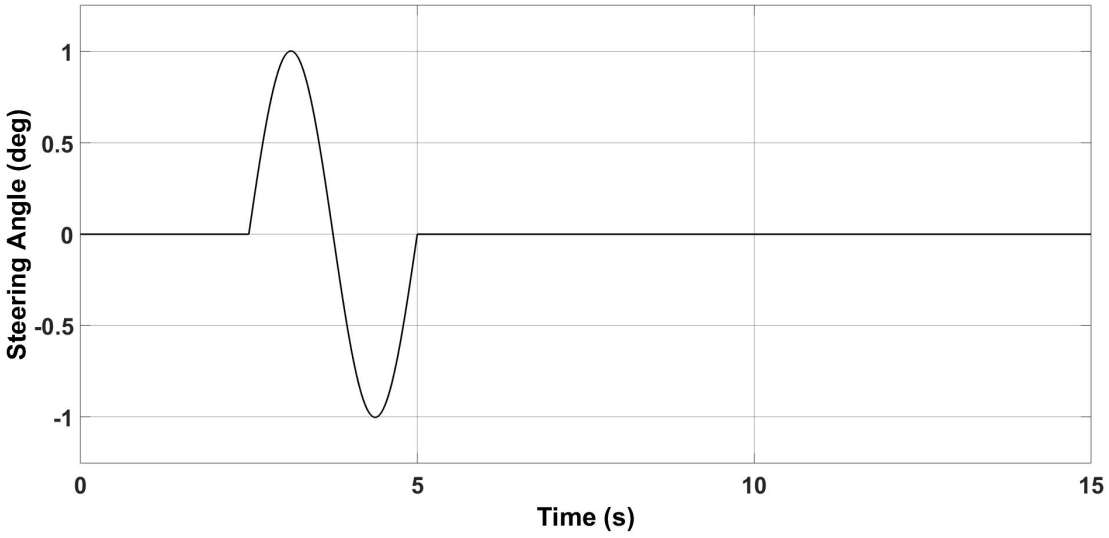

FIGURE 3.3: Time history of the steering angle input recommended by SAE J2179.

Figures 3.4 and 3.5 show the lateral acceleration and yaw rate responses, respectively. To confirm whether the linear model has similar behaviour to that of the TruckSim (baseline) model, the magnitudes and tendency of the curves

based on the two models are compared. All curves seen in Figures 3.4 and 3.5 show good agreement between the linear and nonlinear models. Although the linear model shows good agreement with the nonlinear model, it can be noted that the nonlinear model exhibits higher peak values of lateral accelerations, and requires longer settling times after completing the SLC. Overall, both models respond similarly to the same steering input. It is believed that the 4-DOF yaw-plane model can be used for the design of the ATS controllers.

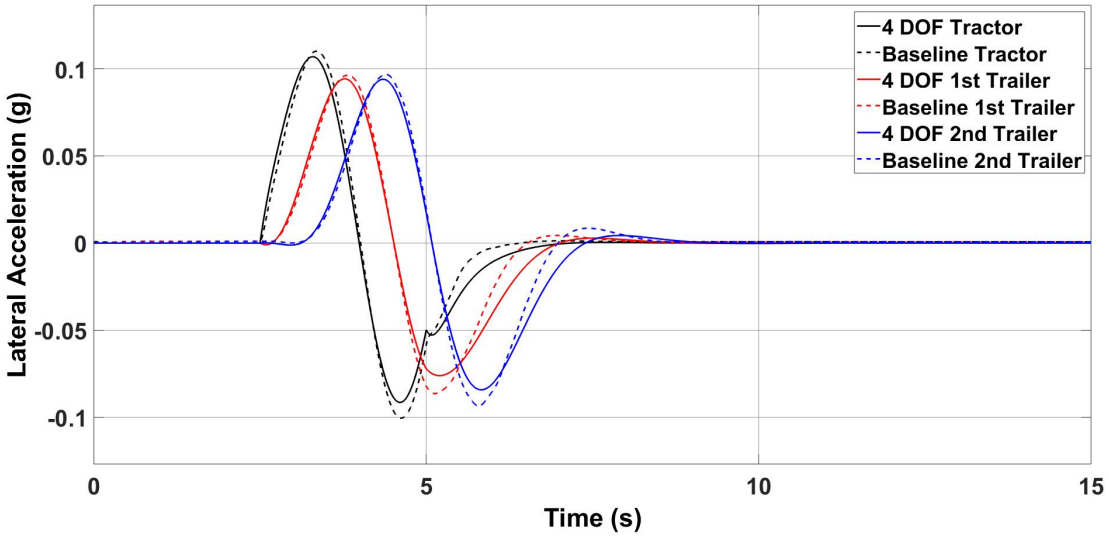

FIGURE 3.4: Time history of lateral accelerations of the 4-DOF and TruckSim (baseline) models.

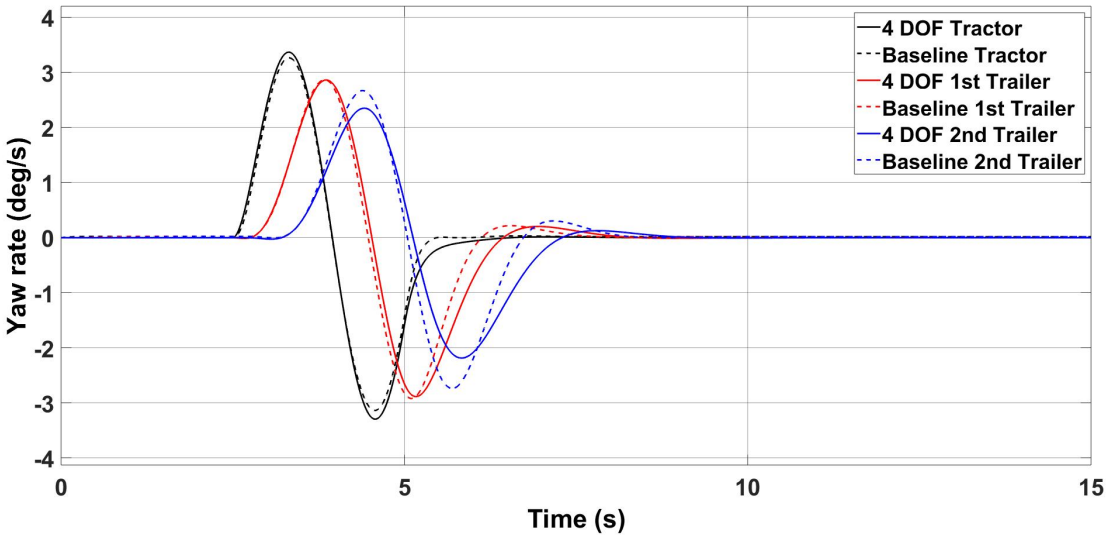

FIGURE 3.5: Time history of yaw rates of the 4-DOF and TruckSim (baseline) models.

3.4 Eigenvalue Analysis

In this section, the stability boundaries of the B-Train Double are examined using eigenvalue analysis based on the linear 4-DOF yaw-plane model. The eigenvalue analysis is conducted to identify the stability boundary in terms of critical speed, above which the vehicle will lose the lateral stability [78]. To perform the eigenvalue analysis, the system matrix A of the 4-DOF model shown in Equation 3.10 is utilized to compute the eigenvalues of the vehicle system.

The eigenvalues of a linear dynamic system are complex numbers and can be expressed as,

$$S_{1,2} = R_e \pm j\omega_d \tag{3.12}$$

where, R_e and $j\omega_d$ represent the real and imaginary parts, respectively. The complex number is then used to calculate the damping ratio (ζ). The damping

ratio is a function of forward speed to identify the critical speed, and can be expressed as,

$$\zeta = \frac{-R_e}{\sqrt{(R_e)^2 + (\omega_d)^2}} \tag{3.13}$$

The damping ratio varies between -1 and 1. The system is considered to be stable if all the motion modes of the system have a damping ratio within the range of $1 \geq \zeta > 0$. Otherwise, if the damping ratio is within the range of $0 > \zeta \geq -1$, the respective motion mode is deemed to be unstable.

To design and synthesize an effective and efficient controller, it is essential to have an accurate estimation of the critical vehicle parameters and their impact on the system performance. To this end, the eigenvalues with different trailer payloads are conducted and analyzed to better understand the respective effects on the system dynamic behaviour. To cover a wide range of payload variation, three payload cases are considered: 1) empty trailer payload with 0.0 kg weight, 2) medium trailer payload with 10,000 kg weight, and 3) full trailer payload with 26,000 kg weight. It is noteworthy mentioning that the maximum allowed trailer payload by the MTO is 26,000 kg [2]. Figures 3.6 -3.8 illustrate the damping ratio of the B-Train Double considering the payload variation.

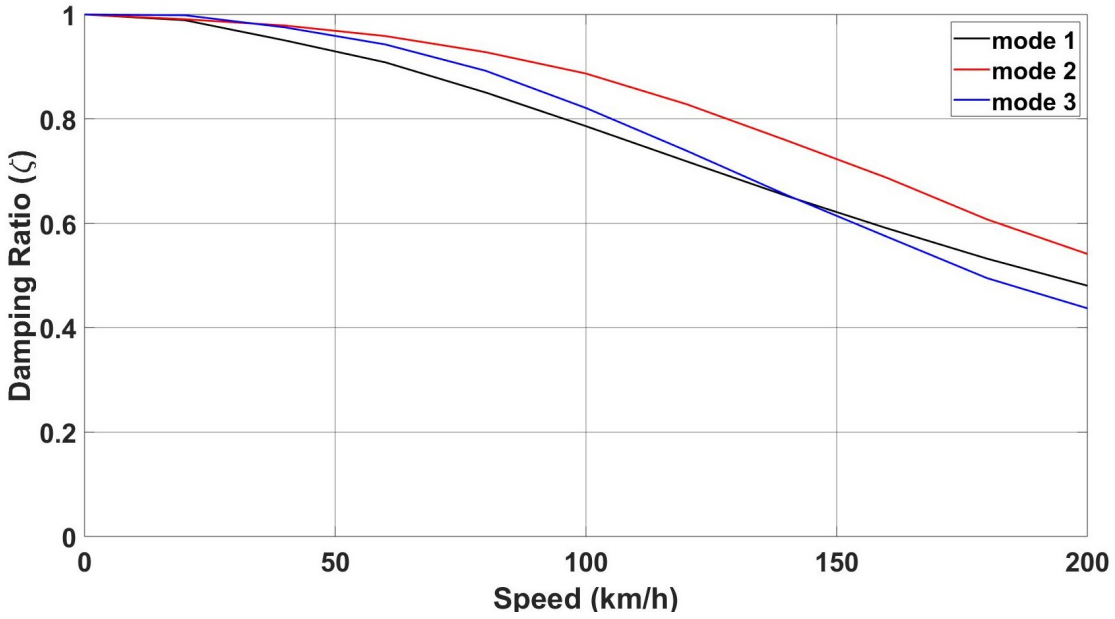

FIGURE 3.6: Damping ratio for the case of empty trailer payload.

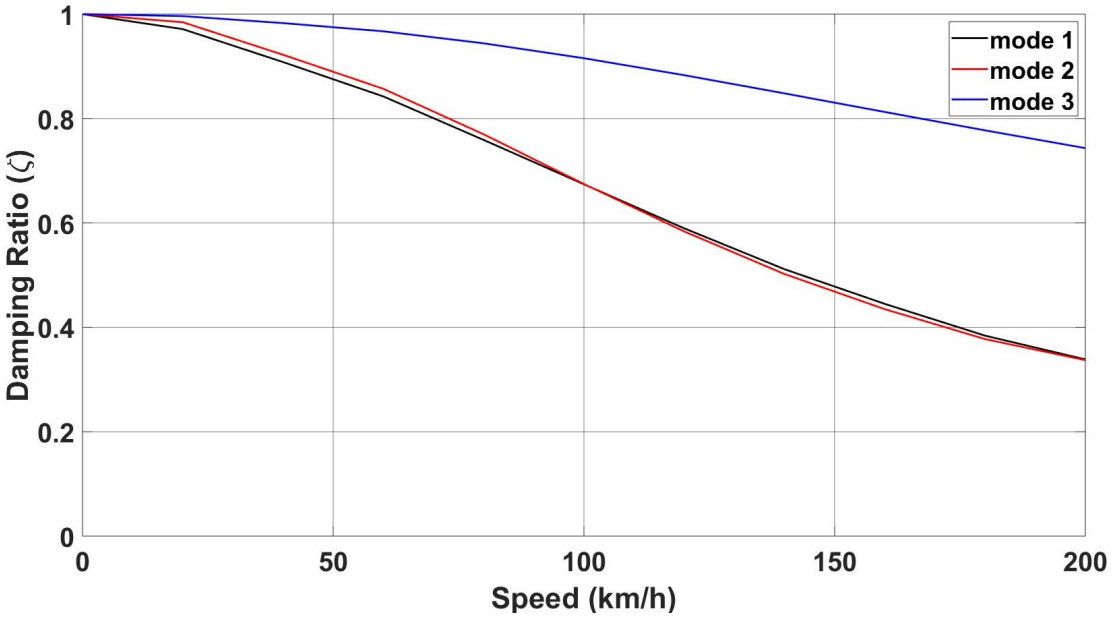

FIGURE 3.7: Damping ratio for the case of medium trailer payload.

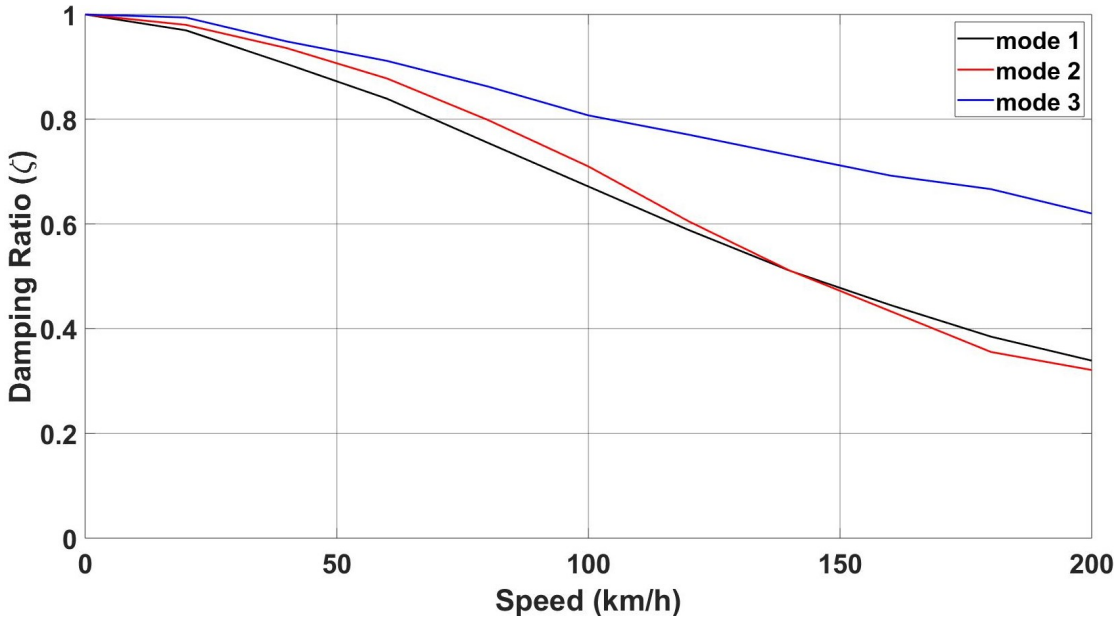

FIGURE 3.8: Damping ratio for the case of full trailer payload.

The results shown in Figures 3.6 - 3.8 reveal the following facts: 1) with a given trailer payload, the damping ratio decreases with the increase of the vehicle forward speed, and 2) for the motion mode with the least damping ratio, this ratio decreases with the increase of the trailer payload. Compared with the case of empty trailer payload, in the case of full trailer payload, the damping ratio of motion modes 1 and 2 reduces by about 31% and 40%, respectively. The above-observed facts are consistent with the observations by Fancher and Winkler [12].

3.5 Controllers Design

Based on the linear 4-DOF yaw-plane model derived and validated in Sections 3.3 and 3.4, two ATS controllers are designed using the LQR and LMI+LQR techniques, respectively.

3.5.1 LQR-based Controller

To design the LQR-based controller for the ATS system, the linear 4-DOF yaw-plane model described in Equation 3.10 should be augmented to include the term associated with the control variables. The augmented state-space representation of the vehicle system model is formulated as,

$$\dot{\mathrm{x}}(\mathrm{t}) = Ax(t) + Bu + C\delta(t) \tag{3.14}$$

where B is the control matrix, and u denotes the control variable vector, which is defined as

$$u = [\delta_4 \quad \delta_5 \quad \delta_6 \quad \delta_7 \quad \delta_8 \quad \delta_9]^T \tag{3.15}$$

where δ_4 to δ_9 represent the steering angle of the wheel on the first axle of the first trailer to the steering angle of the wheel on the last axle of the second trailer, respectively. The design of the LQR-based controller can be described as an optimization problem: minimize the objective function or performance index

$$J = \int_0^\infty (x^T Q x + u^T R u) dt \tag{3.16}$$

subject to Equation 3.14, where Q and R are the weighting matrices. The selection of the element values of the weighting matrices will impose penalties upon the magnitude and duration of the state and control variables. The solution to the optimization problem can be achieved by solving the algebraic Riccati equation,

$$A^T P + PA - PBR^{-1}B^T P + Q = 0 \tag{3.17}$$

where P is the 6x6 definite symmetric matrix. The feedback control gain is determined by,

$$K = R^{-1} B^T P \tag{3.18}$$

and the control variable vector is given by,

$$u(t) = -Kx(t) \tag{3.19}$$

Substituting Equation 3.19 into Equation 3.14, we can obtain the equivalent system matrix as,

$$A_{controlled} = A - BK \tag{3.20}$$

Manual tuning using the trial and error method is carried out to determine the element values of both the weighting matrices of Q and R. To validate the LQR-based controller, a closed-loop SLC maneuver is performed using the TruckSim and MATLAB/Simulink co-simulation as illustrated in Figure 3.9. The dynamic responses of the LQR-based ATS system is discussed in Chapter 4.

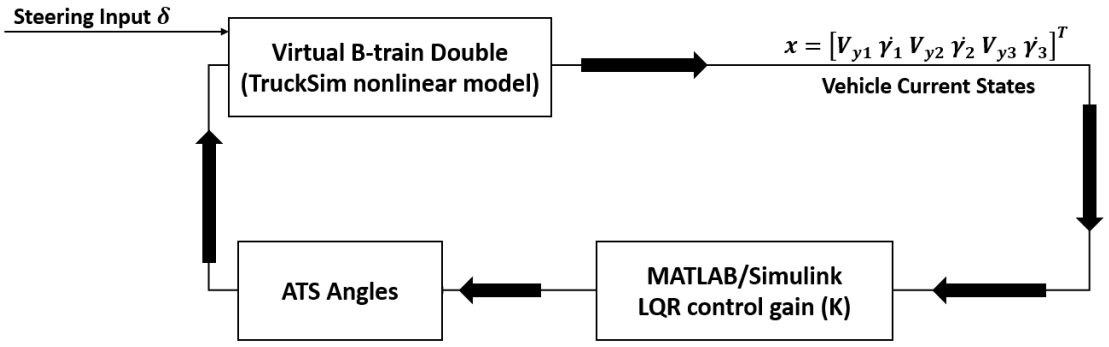

FIGURE 3.9: Co-simulation environment with MATLAB-TruckSim for Implementing the LQR-based ATS controller.

3.5.2 LMI+LQR-based Controller

In the design of the LQR-based controller, all the system parameters are assumed to be constant. For example, the vehicle payload and forward speed are kept constant. However, in a real-life system, there exist system uncertainties, and therefore, it is reasonable to question the robustness of the LQR-based controller. To address the robustness problem of the LQR-based controller, the LMI+LQR-based controller is proposed. The proposed robust controller is designed by combining the LMI and LQR techniques. The combined technique is utilized to design the ATS controller considering the trade-off between the robust performance and the complexity of the resulting control system [79].

To design a robust control system, it is crucial to identify essential uncertainties, which occur in the operation of the dynamic system. In this research, two types of uncertainties are considered: 1) dynamic parameters of trailer steering actuator, and 2) variations of vehicle model parameters. To explore the effects of dynamic parameters of trailer steering actuators, the ATC, $T_a \in [\,T_{a_{min}} \quad T_{a_{max}}]$, is selected as one uncertainty; to study the influences of vehicle model parameter variations, the payload of the trailers, $m_t = m_{t1} = m_{t_2} \in [m_{t\,min} \quad m_{t\,max}]$, is chosen as another uncertainty.

The augmented state-space model with polytopic uncertainties is formulated by combining the ATS actuator model with the 4-DOF linear model and considering the parametric uncertainties. The augmented state-space is represented as,

$$\dot{\tilde{\mathrm{x}}} = \tilde{A}(m_t, T_a)\tilde{x} + \tilde{B}(m_t, T_a)u_1 + \tilde{C}(m_t)\delta \tag{3.21}$$

where,

$$T_a \in [T_{a_{min}} \quad T_{a_{max}}]$$

$$m_t = m_{t1} = m_{t_2} \in [m_{t\,min} \quad m_{t\,max}]$$

$$\tilde{x} = [V_{y1} \quad \dot{\gamma}1 \quad V_{y2} \quad \dot{\gamma}2 \quad V_{y3} \quad \dot{\gamma}_3 \quad u]^T$$

$$u_1 = -K\tilde{x} \tag{3.22}$$

The LMI+LQR-based control formulation is adapted from [21, 24, 80]. The LMI+LQR-based controller is designed using the LMI and LQR Control Toolbox in MATLAB.

Figure 3.10 illustrates the block diagram for the closed-loop simulation for the B-Train Double with the robust LMI+LQR-based ATS controller.

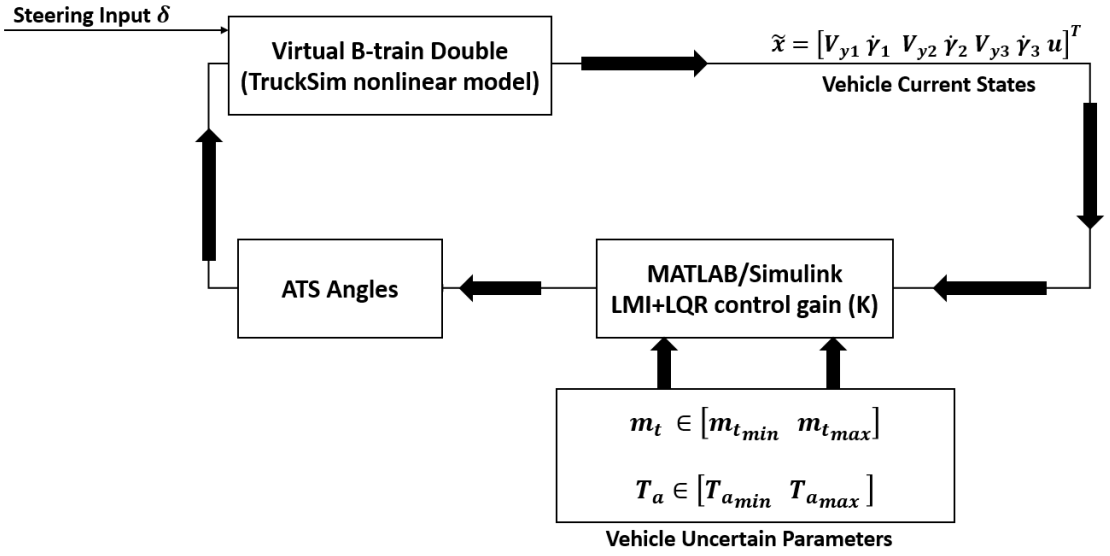

FIGURE 3.10: Co-simulation environment with MATLAB-TruckSim for Implementing the LMI+LQR-based ATS controller.

3.5.3 Definition of Uncertain Parameters

The B-Train Double is a complex system subject to various parameter uncertainties, e.g., different payloads, forward speeds, and CG locations. In this

thesis, the trailers payload variation and trailer steering ATC are selected as parametric uncertainties to test the response and robustness level of the LQR- and LMI+LQR-based controllers. To examine the effect of the trailers payload variation on the system stability and robustness of the controllers, four different payload scenarios are considered: 1) 0.0 kg, 2) 10,000 kg, 3) 15,000 kg, and 4) 26,000 kg. It is noteworthy mentioning that some parameters change with respect to the payload variation, e.g., the tire cornering stiffness and the trailer moment of inertia.

The second uncertain parameter is the ATS ATC. The actuator dynamic performance can be simplified using the following model [20, 24, 81]:

$$G_a = \frac{1}{T_a s + 1} \tag{3.23}$$

where T_a denote the ATC, the time constant T_a affects the reaction speed of the actuator; if the actuator is responsive, T_a will take a small value, otherwise, T_a could take a large value in the case of a slow actuator. To test the robustness of the controller subject to a varied range of the ATS ATC, the variation range is selected to change from 0 to 2 second with an increment of 0.5 second. Once the actuator uncertainty is considered to be part of the ATS system, Figure 3.9 is updated to incorporate the ATC into the co-simulation environment combining MATLAB/Simulink and TruckSim, as shown in Figure 3.10.

In the closed-loop co-simulation environment shown in Figures 3.9 and 3.10, a virtual driver is used to follow the desired SLC path. Under the simulated maneuver, the driver model adjusts the steering input of the tractor to track the predefined trajectory [25].

3.6 Summary

This chapter describes the design of two ATS controllers. First, a 4-DOF yaw-plane model is derived using the Newton-Euler method. The dynamic responses of the 4-DOF linear model are then validated against the TruckSim nonlinear model, under an open-loop SLC maneuver specified by SAE J2179. Simulation results indicate that the linear and nonlinear models achieve good agreement, and the linear model is justified to be used for the design of the ATS controllers. For the preparation of the design of the ATS controllers, eigenvalues analysis is carried out to estimate the stable boundaries of the system under varying trailer payloads. The achieved results show that the linear model maintains stability under three different payloads.

Once the linear model is validated, and the stability boundaries are examined, the two ATS controllers are designed to enhance the lateral stability of the B-Train Double at high speeds. The first ATS controller is devised using the LQR technique, while the second is designed by combining the LMI and LQR techniques. Lastly, two parametric uncertainties are introduced to test the robustness of the proposed controllers.

Chapter 4

Results and Discussion

4.1 Introduction

In order to evaluate the performance of the proposed ATS controllers, a virtual TruckSim driver is used to perform a closed-loop SLC maneuver. The controllers designed in MATLAB/Simulink are linked to the nonlinear model vehicle model developed in TruckSim using an interface, namely S-function. A block diagram describing the closed-loop environment is depicted in Figure 3.9. The virtual driver is responsible for following the predefined trajectory for the SLC maneuver. In this chapter, the TruckSim (baseline) model is used as the virtual vehicle to examine the robustness of the proposed ATS controllers under three scenarios.

The three scenarios are specified as 1) under the condition of varying trailers' payload and absence of ATS ATC, the dynamics of the baseline vehicle without ATS is compared with those of the vehicle with the LQR- and LMI+LQR-based controller, 2) under the condition of varying trailers payload and constant ATS ATC, the performance of the LQR-based controller is compared with

that of the LMI+LQR-based controller, and 3) under the condition of constant trailers payload and varying ATS ATC, the performance of the LQR-based controller is compared with that of the LMI+LQR-based controller. Built upon the above benchmark study, the limitation of the LQR-based controller is discussed. Lastly, the LMI+LQR-based controller is validated using the HIL-RT simulations executed on the driving simulator at the University of Ontario Institute of Technology (UOIT).

4.2 Performance of LQR- and LMI+LQR-based Controllers

4.2.1 Results Achieved Under First Scenario

In this subsection, the payload of the trailers is a variable, and the ATC Ta is neglected. Four different trailer payloads are considered: 1) 0.0 kg payload weight, 2) 10,000 kg payload weight, 3) 15,000 kg payload weight, and 4) 26,000 kg payload weight. The design objective of the ATS controllers is to achieve an RWA ratio of 1.0, thereby ensuring superior lateral stability and good PFOT at high speeds. Under the closed-loop SLC maneuver specified by ISO-14791:2000(E) [82], the virtual vehicle travels at the forward speed of 100 km/h, and the virtual driver continuously adjusts the steering input to allow the vehicle to trace the prescribed path. Under the specified scenario and simulated testing maneuver, the dynamics of the baseline vehicle without ATS is compared with those of the vehicle with the LQR- and LMI+LQR-based controller.

In Case 1, the trailers payload is set to be 0.0 kg. Figures 4.1 and 4.2 show the lateral acceleration and yaw rate responses of the vehicle without ATS and with the LQR-based controller, respectively.

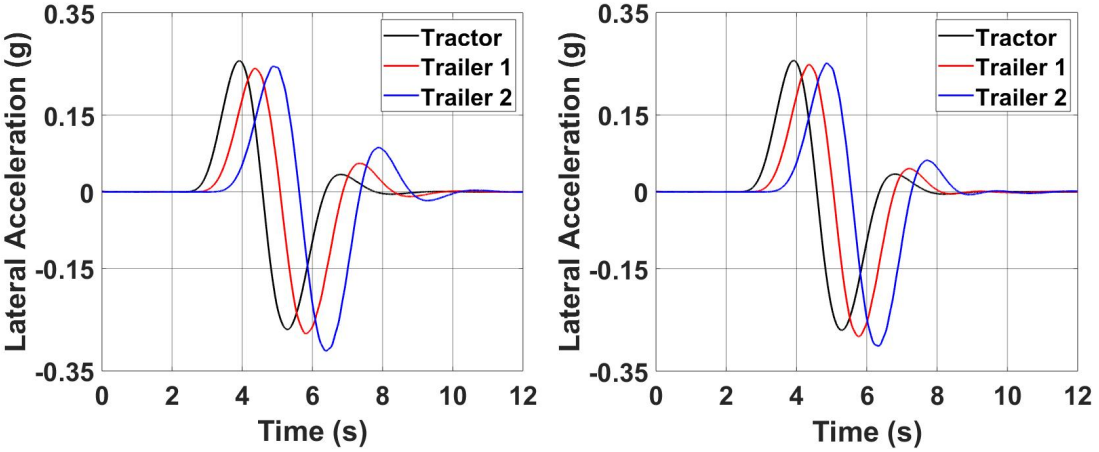

(a) (b)

FIGURE 4.1: Time histories of lateral acceleration for the B-Train Double (a) without ATS, and (b) LQR-based ATS controller.

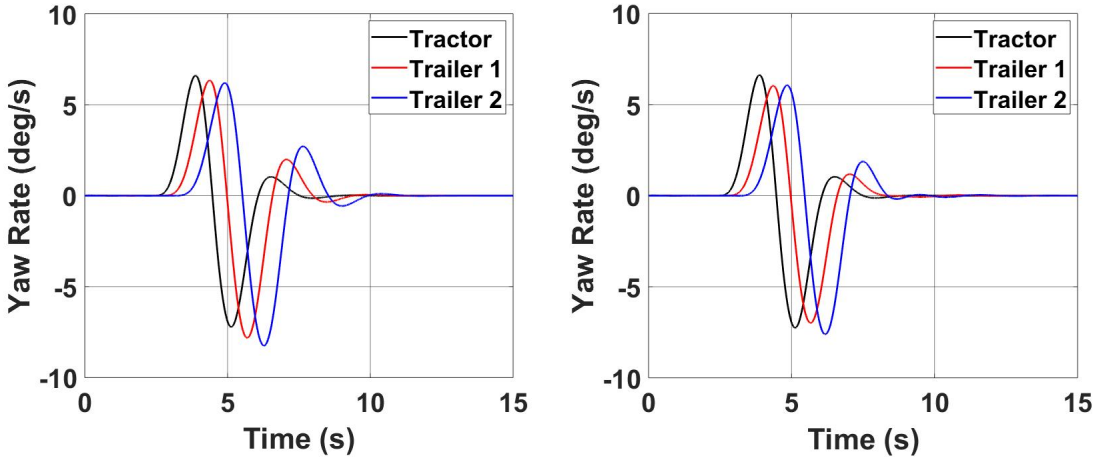

(a) (b)

FIGURE 4.2: Time histories of yaw rate for the B-Train Double (a) without ATS, and (b) LQR-based ATS controller.

As seen in Figure 4.1, the LQR-based controller reduces the RWA ratio by about 3.6% compared against that of the baseline case. In addition, the LQR-based

controller reduces the second trailers settling time. As shown in Figure 4.2, the LQR-based controller makes the peak values of the trailers yaw rate smaller than those of the baseline case. Moreover, as seen in Figures 4.1 and 4.2, the LQR-based controller makes the ripples of lateral acceleration and yaw rate of the vehicle units smaller than those of the baseline case.

In addition to the improvement of the lateral stability, the LQR-based controller can also enhance the PFOT of the vehicle. Figure 4.3 shows the trajectories of all vehicle units over the simulated SLC maneuver, along with the the predefined trajectory for reference.

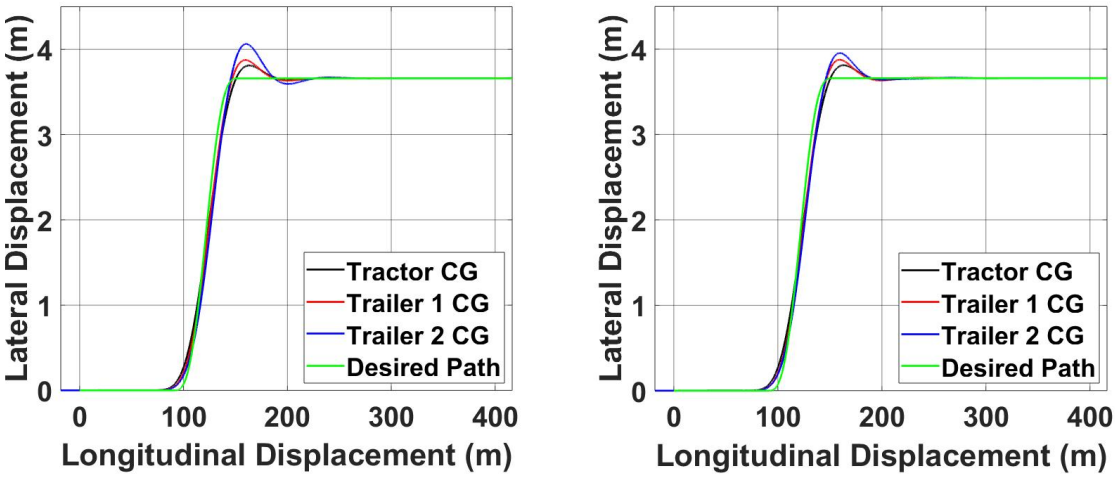

FIGURE 4.3: Trajectories of the vehicle units for B-Train Double (a) without ATS, and (b) LQR-based ATS controller.

Similarly, under the closed-loop SLC maneuver with the condition of the trailers payload of 0.0 kg (case 1) from Table 4.1, Figures 4.4 and 4.5 show the lateral acceleration and yaw rate responses of the vehicle without ATS and with the LMI+LQR-based controller, respectively.

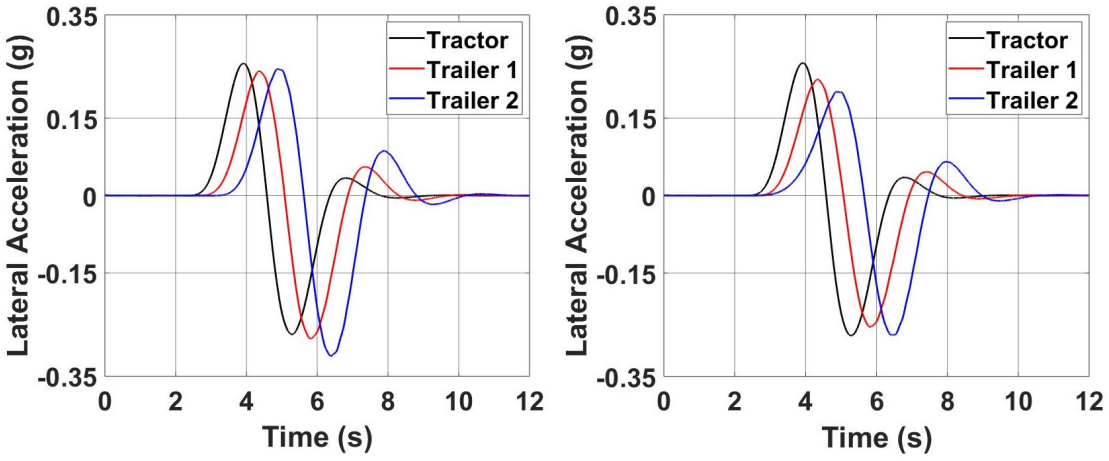

(a) (b)

FIGURE 4.4: Time histories of lateral acceleration for the B-Train Double (a) without ATS, and (b) LMI+LQR-based controller.

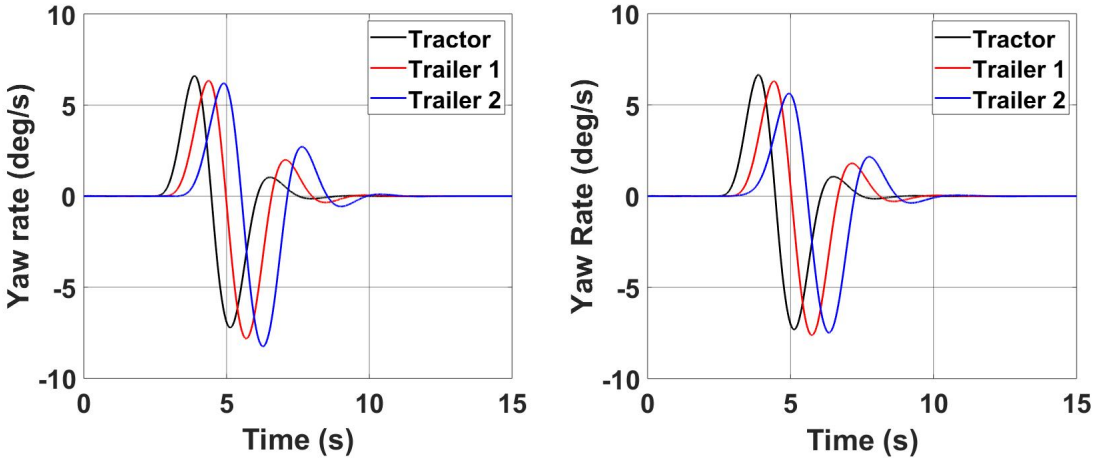

(a) (b)

FIGURE 4.5: Time histories of yaw rate for the B-Train Double (a) without ATS, and (b) LMI+LQR-based controller.

As shown in Figures 4.4 and 4.5, the LMI+LQR-based controller reduces the maximum peak values of the trailers in the lateral acceleration and yaw rate. It is observed that the LMI+LQR-based controller reduces the RWA ratio by 13% compared against that of the baseline case.

Figure 4.6 shows the trajectories of all vehicle units achieved under the simulated closed-loop maneuver for case 1. Compared with the baseline case, the LMI+LQR-based controller reduces the overshoot of the trajectory for the second trailer, thereby improving the PFOT of the vehicle.

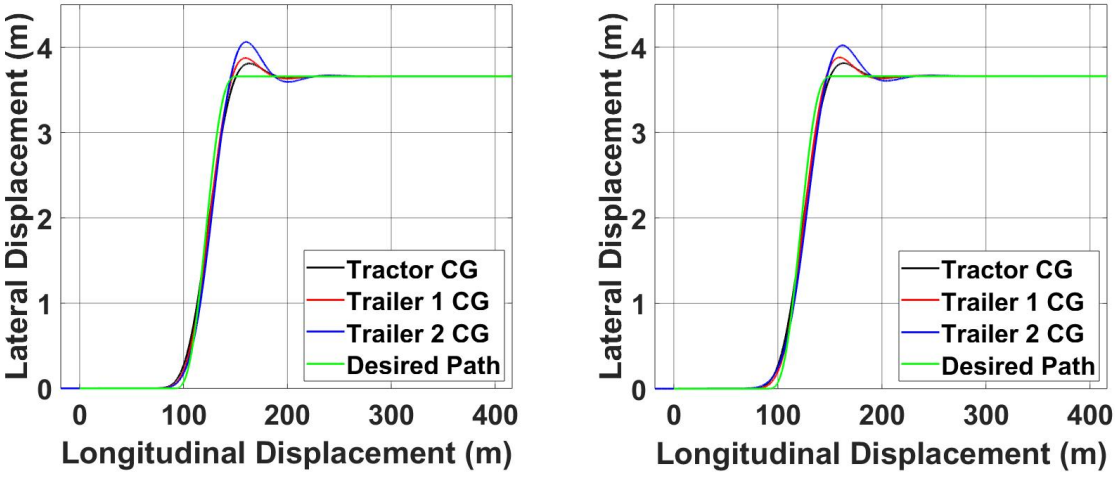

(a) (b)

FIGURE 4.6: Trajectories of the vehicle units for B-Train Double (a) without ATS, and (b) LMI+LQR-based controller.

Figures 4.1 - 4.6 only show the results achieved under the simulated closed-loop SLC maneuver at 100 km/h with trailers payload of 0.0 kg (case 1) from Table 4.1. The simulation results for the other three cases (i.e., with different trailers payloads) are provided in Appendix A.1. To summarize the RWA measure for the baseline, the LQR-based controller, and the LMI+LQR-based controller, Table 4.1 lists the quantitative simulation results achieved under the SLC maneuver at 100 km/h for all the four trailers payload cases. Figure 4.7 visualize the results listed in Table 4.1 in terms of the relationship between the RWA measure and trailers payload. It is observed that for all the cases of baseline,

LQR- and LMI+LQR-based controllers, the RWA measure varies with the trailers payload in similar tendency, that is, the RWA ratio increases with the trailers payload. This tendency is consistent with the simulation results based on the eigenvalue analysis, as shown in Figures 3.6 - 3.8. As seen in Figure 4.7, among the three cases of baseline, LQR- and LMI+LQR-based controller, the last case shows the lowest RWA ratio with a given trailers payload. This implies that the LMI+LQR-based controller can achieve the best performance in terms of lateral stability and PFOT.

TABLE 4.1: The RWA measures of the B-Train Double under the closed-loop SLC maneuver with different payloads and constant Ta = 0 s.

Case No.	**Weight (kg)**	**ATC (s)**	**RWA**		
			Baseline	**LQR**	**LMI**
1	0	0	1.1561	1.1142	0.9959
2	10,000	0	1.1663	1.1318	1.0354
3	15,000	0	1.1612	1.1197	1.0567
4	26,000	0	1.166	1.1298	1.0622

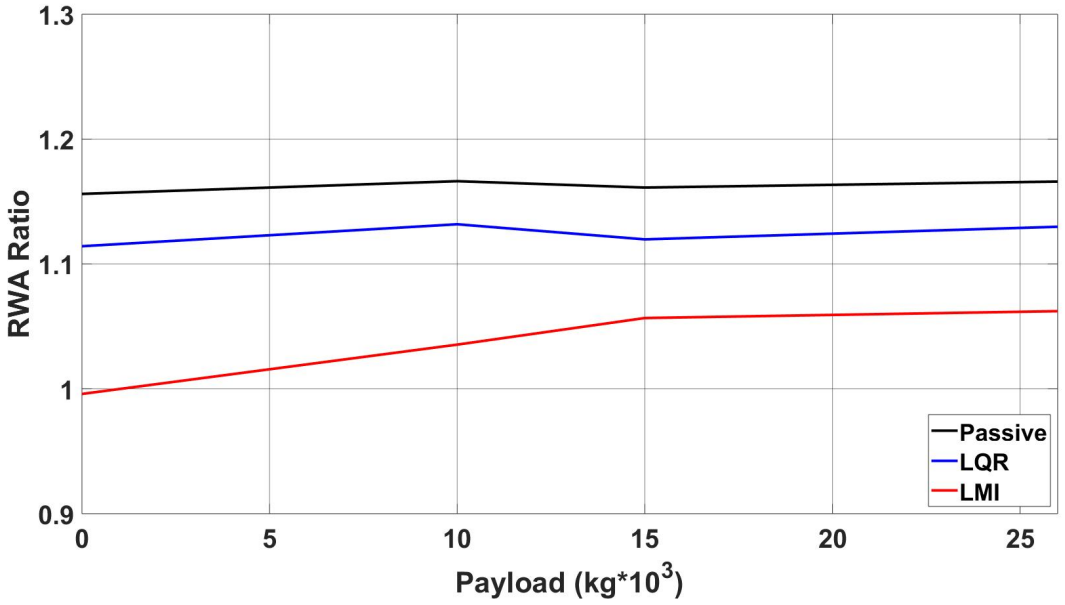

FIGURE 4.7: RWA measure under the variation of trailers' payload.

4.2.2 Results Achieved Under Second Scenario

This subsection evaluates the lateral stability of the B-Train Double with the LQR- and LMI+LQR-based controller. The evaluation is implemented under the simulated closed-loop SLC maneuver at the forward speed of 100 km/h. In the evaluation, four cases are considered, for which the ATS ATC takes the value of 0.5, 1.0, 1.5, and 2.0 second, respectively. The corresponding cases are denoted as A, B, C, and D. For each case, the trailers payload takes the value of 0, 10,000, 15,000, and 26,000 kg. Table 4.2 lists the quantitative simulation results in terms of the RWA measure for the four cases.

Figure 4.8 shows the lateral acceleration responses of the vehicle with the LQR- and LMI+LQR-based controller for Case B with trailers payload of 10,000kg. As seen in Figure 4.8, the LQR-based controller shows a higher lateral acceleration peak value at the CG of the second trailer compared against the case of

LMI+LQR-based controller. Accordingly, the RWA ratio for the case of LQR-based controller is 1.1925, while the RWA ratio for the case of the LMI+LQR-based controller ATS is 1.0994. In addition, it is observed that compared with the case of the LQR-based controller, the LMI+LQR-based controller makes the ripples of the lateral acceleration smaller and shortens the respective settling times. It should be mentioned that both the cases exhibit high lateral dynamic load transfer, with which the tractors lateral acceleration curve tends to be noisy.

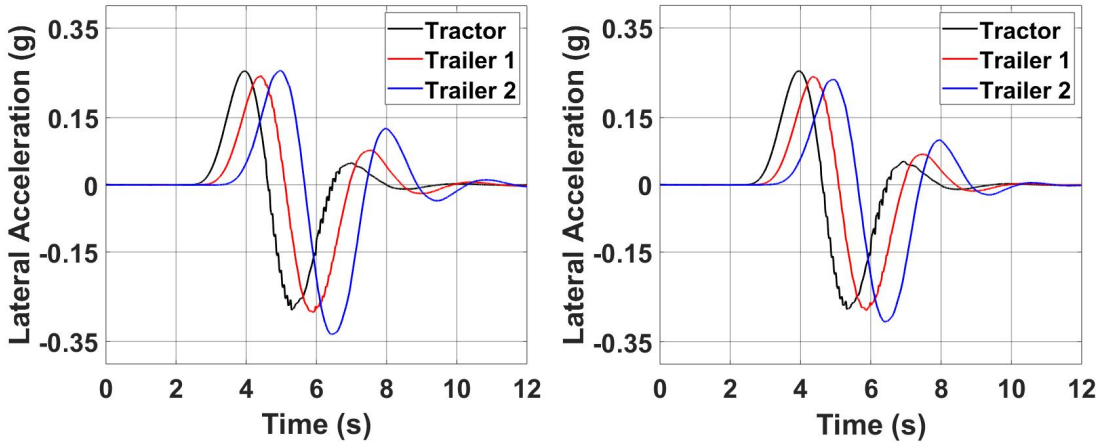

(a) (b)

FIGURE 4.8: Time histories of lateral accelerations of the B-Train Double with case B and trailers payload of 10,000kg: (a) LQR-based controller, and (b) LMI+LQR-based controller.

Figure 4.9 shows the respective trajectories of vehicle units for the cases of the LQR- and LMI+LQR-based controller. Compared with the former, the latter shortens the peal lateral displacement of the second trailer by 6.2%.

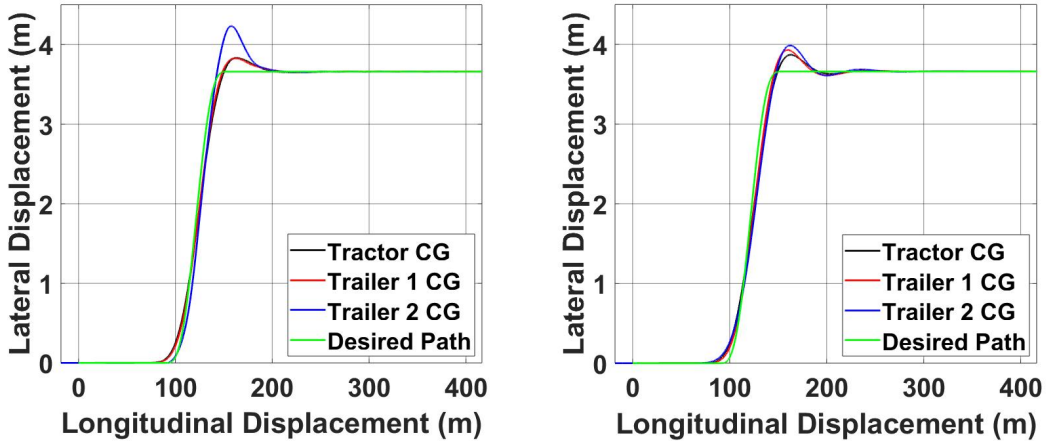

FIGURE 4.9: Trajectories of the vehicle units for B-Train Double with case B and trailers payload of 10,000kg: (a) LQR-based controller, and (b) LMI+LQR-based controller.

Figures 4.8 and 4.9 only show a sample result for case B with trailers payload of 10,000 kg to examine the robustness of the LMI+LQR-based controller. The rest of the simulation results achieved under the second scenario are offered in Appendix A.2. As mentioned previously, Table 4.2 offers the quantitative simulation results achieved under the second scenario.

TABLE 4.2: The RWA measures of the B-Train Double under the closed-loop SLC maneuver with ATC intervals and variation of payload.

Case No.	Weight (kg)	ATC (s)	RWA	
			LQR	LMI
Case A				
1	0	0.5	1.1974	0.9959
2	10,000	0.5	1.1921	0.9808
3	15,000	0.5	1.2282	1.0011
4	26,000	0.5	1.2523	1.1128

Case No.	Weight (kg)	ATC (s)	RWA	
			LQR	LMI
Case C				
1	0	1.5	1.2947	1.1183
2	10,000	1.5	1.3393	1.0311
3	15,000	1.5	1.2248	1.1732
4	26,000	1.5	1.2235	1.1714

Case No.	Weight (kg)	ATC (s)	RWA	
			LQR	LMI
Case B				
1	0	1	1.2114	1.09
2	10,000	1	1.1925	1.0994
3	15,000	1	1.219	1.1422
4	26,000	1	1.2185	1.1536

Case No.	Weight (kg)	ATC (s)	RWA	
			LQR	LMI
Case D				
1	0	2	1.3361	1.1319
2	10,000	2	1.5262	1.1055
3	15,000	2	1.6626	1.1837
4	26,000	2	1.3365	1.199

As shown in Table 4.2, the RWA ratio increases with the increase of trailers payload under a given ATS ATC; with a given trailers payload, the RWA ratio increases with the increase of the ATS ATC. For each case, compared with the case of the LQR-based controller, the LMI+LQR-based controller makes the RWA ratio closer to the desired value of 1.0, indicating that the latter shows robust performance than the former. To better understand the relationship between the RWA measure and the trailers payload, Figure 4.10 shows the sample result for Case D.

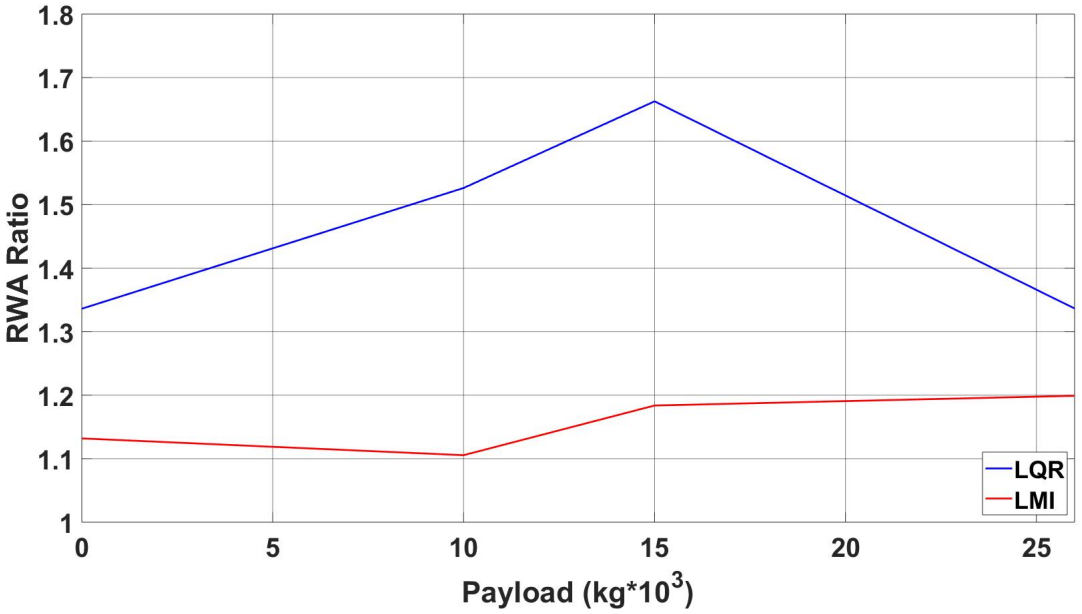

FIGURE 4.10: Case D - RWA measure under constant ATC of two seconds and variation of trailers' payload.

Figure 4.10 highlights the following points: 1) the LMI+LQR-based controller shows an overall consistent tendency, where the RWA ratio increases with the trailers payload, 2) the LQR-based controller experiences an unexpected tendency, where the RWA ratio increases with the trailers payload and the ratio reaches its peak value at the trailers payload of 15,000 kg, then it reduces with the increase of the trailers payload, and 3) with a given trailers payload, the RWA ratio for the case of LMI+LQR-based controller is smaller and closer to the desired value of 1.0 compared against that for the case of LQR-based controller.

4.2.3 Results Achieved Under Third Scenario

This subsection assesses the lateral stability of the B-Train Double with the LQR- and LMI+LQR-based controller. The assessment is executed under the simulated closed-loop SLC maneuver at the forward speed of 100 km/h. In the

assessment, four cases are considered, for which the trailers payload takes the value of 0.0, 10,000, 15,000, and 26,000 kg, respectively. The respective cares are denoted as A, B, C, and D. For each case, the ATS ATC takes the value of 0.5, 1.0, 1.5, and 2.0 second. Table 4.3 lists the quantitative simulation results in terms of the RWA measure for the four cases. Figure 4.11 illustrates the lateral acceleration responses of the B-Train Double with the LQR- and LMI+LQR-based controller for Case A with the ATS ATC of 2.0 second, as shown in Table 4.3. The rest of the simulation results listed in Table 4.3 are shown in Appendix A.3.

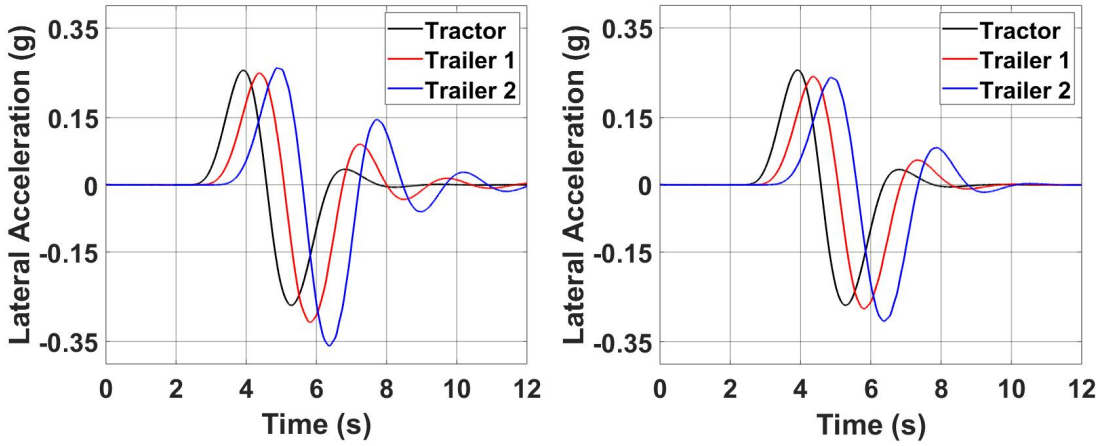

(a) (b)

FIGURE 4.11: Time history of lateral accelerations for the B-Train Double with trailers payload of 0.0 kg, the ATS ATC of 2.0 second, and with: (a) LQR-based controller, and (b) LMI+LQR-based controller.

As seen in Figure 4.11, compared with the case of the LQR-based controller, the LMI+LQR-based controller makes the maximum peak values of trailers lateral accelerations smaller, resulting in reducing the RWA ratio by 18% compared against that of the LQR-based controller. Figure 4.12 shows the respective trajectories of the vehicle units over the closed-loop SLC maneuver. As shown in

Figure 4.12, both controllers achieve similar PFOT. However, the LMI+LQR-based case shows smaller ripple of the trajectories with less settling times compared against those of the LQR-based controller.

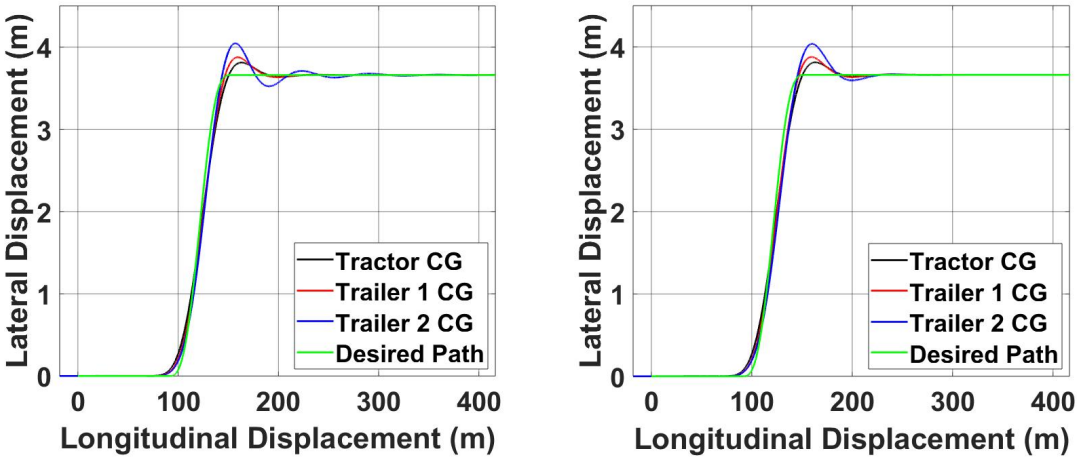

FIGURE 4.12: Trajectories of the vehicle units for B-Train Double with trailers payload of 0.0 kg, the ATS ATC of 2.0 second, and with: (a) LQR-based controller, and (b) LMI+LQR-based controller.

TABLE 4.3: The RWA measures of the B-Train Double under the closed-loop SLC maneuver with constant trailers payload and varying ATS ATC.

Case No.	Weight (kg)	ATC (s)	RWA	
			LQR	LMI
Case A				
1	0	0	1.1142	0.9959
2	0	0.5	1.1974	0.9959
3	0	1	1.2114	1.09
4	0	1.5	1.2947	1.1183
5	0	2	1.3361	1.1319

Case No.	Weight (kg)	ATC (s)	RWA	
			LQR	LMI
Case C				
1	15,000	0	1.1197	1.0567
2	15,000	0.5	1.2282	1.0011
3	15,000	1	1.219	1.1422
4	15,000	1.5	1.2248	1.1732
5	15,000	2	1.6626	1.1837

Case No.	Weight (kg)	ATC (s)	RWA	
			LQR	LMI
Case B				
1	10,000	0	1.1318	1.0354
2	10,000	0.5	1.1921	0.9808
3	10,000	1	1.1925	1.0994
4	10,000	1.5	1.3393	1.0311
5	10,000	2	1.5262	1.1055

Case No.	Weight (kg)	ATC (s)	RWA	
			LQR	LMI
Case D				
1	26,000	0	1.1298	1.0622
2	26,000	0.5	1.2523	1.1128
3	26,000	1	1.2185	1.1536
4	26,000	1.5	1.2235	1.1714
5	26,000	2	1.3365	1.199

As shown in Table 4.3, it is observed that with a given trailers payload, increasing the ATS ATC results in a higher RWA ratio. Both controllers exhibit a similar trend, although the magnitude of the RWA ratio for the LMI+LQR-based controller is smaller than that of the LQR-based controller. To further analyze the results shown in Table 4.3, Figure 4.13 presents the relationship between the RWA ratio and the ATS ATC Ta at the trailers payload of 26,000 kg (i.e., Case D shown in Table 4.3). As shown in Figure 4.13, the curve for the case of

LMI+LQR-based controller is below that for the LQR-based controller, implying that the former achieves better directional performance than the latter.

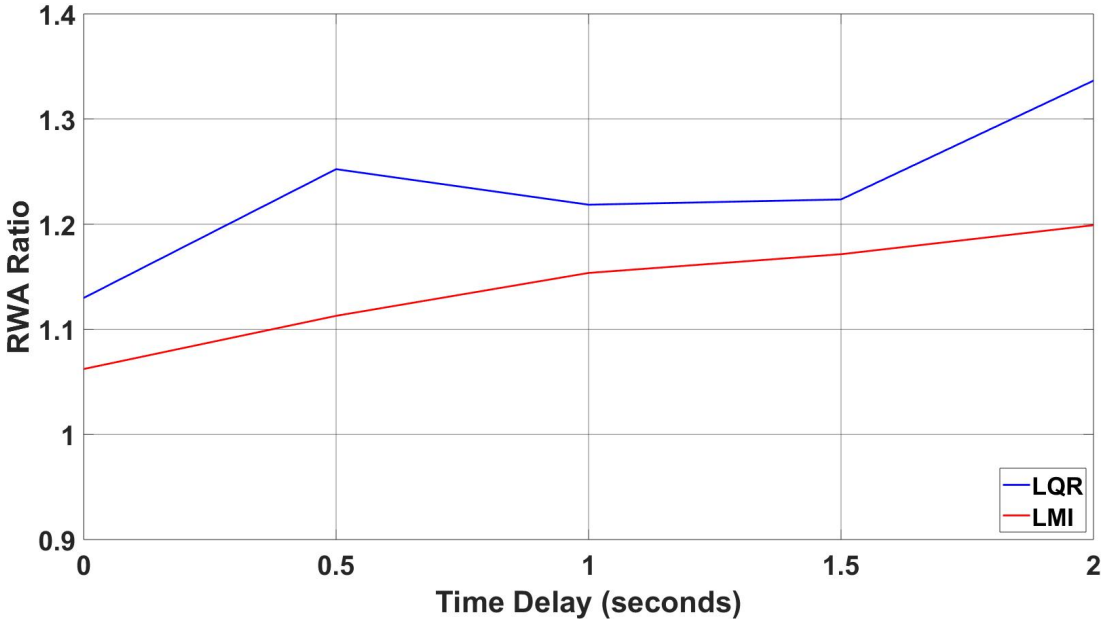

FIGURE 4.13: Case D - RWA measure under constant payload of 26,000 kg and variation of ATC.

4.3 Limitations of LQR-based controller

As discussed in subsection 4.2.1, under the condition of neglecting the ATS ATC, the LQR-based controller shows an improvement in the lateral stability of the B-Train Double. However, once the ATS ATC is considered, the performance of the LQR-based controller may be degraded as discussed in subsection 4.2.3. In this subsection, the performance of the LQR-based controller is further examined and compared against that of the LMI+LQR-based controller under a severe scenario.

The severe scenario is specified as follows. The ATS ATC and the trailers payload takes the value of 2.0 second and 26,000 kg, respectively. Over the closed-loop SLC maneuver, the vehicle travels at the forward speed of 120 km/h.

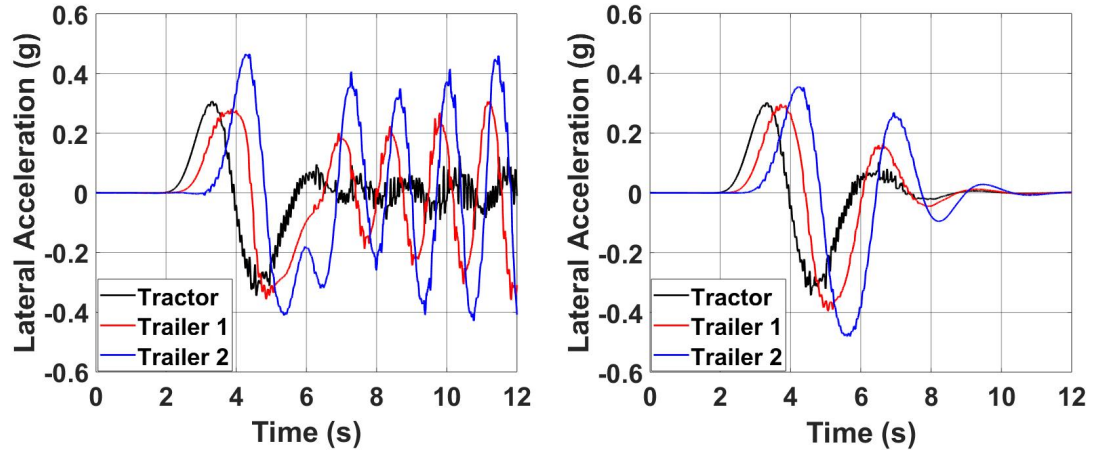

(a) (b)

FIGURE 4.14: Time history of lateral accelerations for vehicle units of the B-Train Double with (a) the LQR-based controller, and (b) LMI+LQR-based controller under the severe scenario.

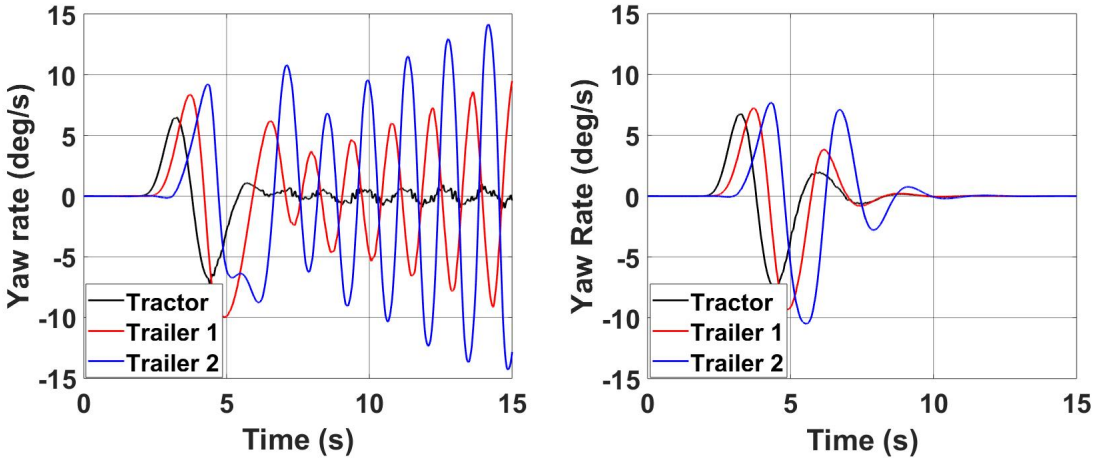

(a) (b)

FIGURE 4.15: Time history of yaw rates for vehicle units of the B-Train Double with (a) the LQR-based controller, and (b) LMI+LQR-based controller under the severe scenario.

Figures 4.14 and 4.15 show the lateral acceleration and yaw rate responses of the vehicle with the LQR- and LMI+LQR-based controllers under the simulated SLC maneuver. As shown in Figures 4.14 (a) and 4.15 (a), as time goes, the magnitude of the lateral acceleration and yaw rate for both the trailers increases,

implying that the vehicle will lose the lateral stability in terms of trailer sway. Moreover, the LMI+LQR-based controller showed robust performance, maintaining the vehicle's lateral stability.

Figure 4.16 shows the trajectories of vehicle units of the B-Train Double with the LQR- and LMI+LQR-based controllers. It is evident in the LQR-based controller case, after completing the SLC, the second trailer experiences lateral oscillation, and the oscillation is divergent, unlike the LMI+LQR-based controller where the vehicle maintained reasonable PFOT and the vehicle followed the intended path. The simulation results presented in Figures 4.14 - 4.16 indicate that subject to a large trailer payload and long steering ATC, the performance of the LQR-based ATS controller may be degraded. This implies that the LQR-based ATS controller lacks robustness.

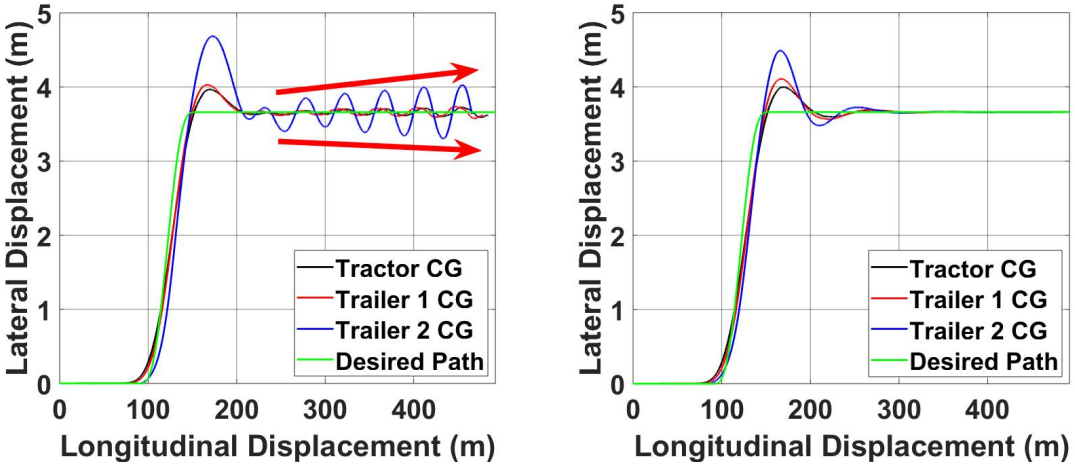

FIGURE 4.16: Trajectories of vehicle units of the B-Train Double with (a) the LQR-based controller, and (b) LMI+LQR-based controller under the severe scenario.

4.4 Validation of LMI+LQR-based Controller Using HIL-RT Simulations

The LMI+LQR-based controller has been examined numerically in terms of the robustness of performance subject to the uncertainties of trailers payload and the ATS ATC. To validate the robust ATS controller for the B-Train Double, Hardware-In-the-Loop Real-Time (HIL-RT) simulations are conducted using the Driver-Hardware-In-the-Loop Real-Time (DHIL-RT) simulator at UOIT. This DHIL-RT simulator has been used to test the controllers, actuators, sensors, and electric control units designed for ATS systems of AHVs [6, 21, 24, 72]. The DHIL-RT simulator consists of a host computer, a LabVIEW-RT computer (i.e., target PC), an electro-hydraulic actuator based ATS axle, an animator computer, and three 46 inch monitors. A Controller Area Network (CAN) and an Ethernet network are used to connect the units mentioned above. The TruckSim and LabVIEW software operating on the host computer are utilized to define and compile the RT B-Train Double and the LMI+LQR-based ATS controller, which are transmitted to the LabVIEW-RT computer. All defined B-Train Double and ATS controller data are also stored on the host computer. The LabVIEW-RT computer runs the B-Train Double model and communicates with the physical ATS axle. In addition, the RT computer may send the vehicle motion data to the animator computer, which provides video feeds to the three monitors.

To evaluate the robust ATS controller, a closed-loop environment is established. The ATS axle equipped with a hydraulic actuator is connected to the DHIL-RT simulator. A steering angle sensor is used to measure the position of the ATS

axle. The physical ATS axle is equipped with a microcontroller, responsible for receiving the simulated ATS angles from TruckSim and comparing it to that of the physical ATS axle. After that, the microcontroller takes action based on the calculated error between the simulated and the measured angles. Once the error is determined, a feedback signal is sent back to the RT computer, resulting in a closed-loop feedback system. Figure 4.17, shows the physical prototype of the ATS axle.

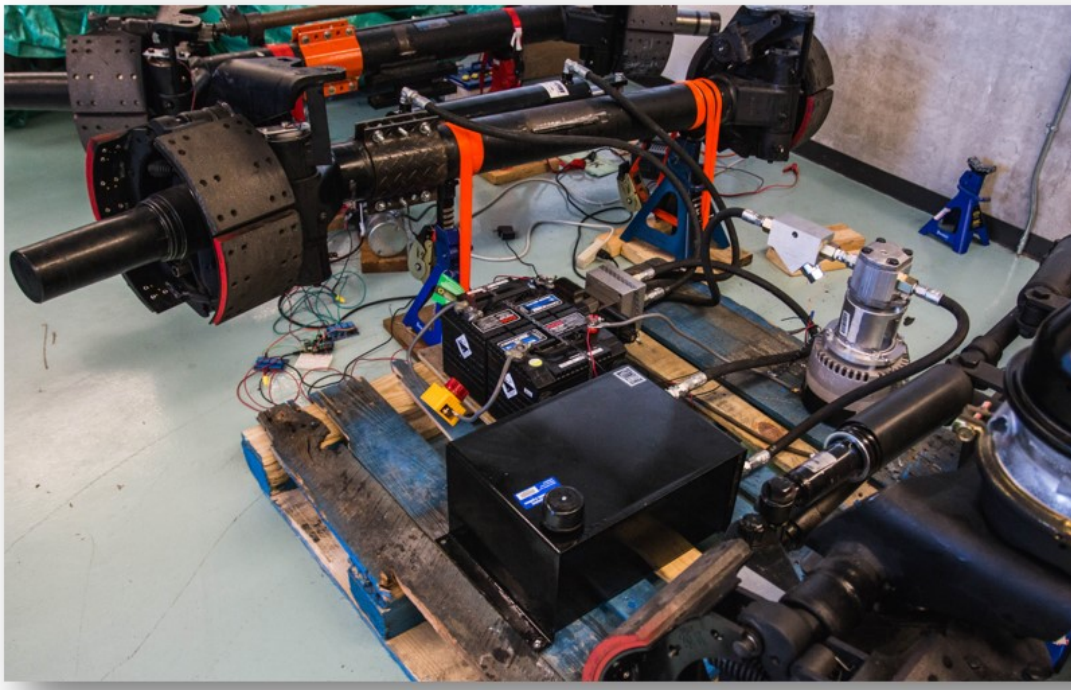

FIGURE 4.17: The physical prototype of the ATS axle.

4.4.1 Robust Controller Performance Validation

To examine the robustness of the LMI+LQR-based controller using HIL-RT simulation, the trailers payload variation is selected as the system uncertainty. In the HIL-RT simulation, the trailers payload takes the value of 0.0, 10,000,

15,000, and 26,000 kg. The HIL-RT simulation is implemented under a closed-loop SLC maneuver at the forward speed of 100 km/h. The achieved HIL-RT simulation results are compared with those based on numerical simulations. Figure 4.18 shows the lateral acceleration responses of the B-Train Double with the robust ATS system obtained from the numerical and HIL-RT simulations, under the closed-loop SLC maneuver with trailers payload of 0.0 kg.

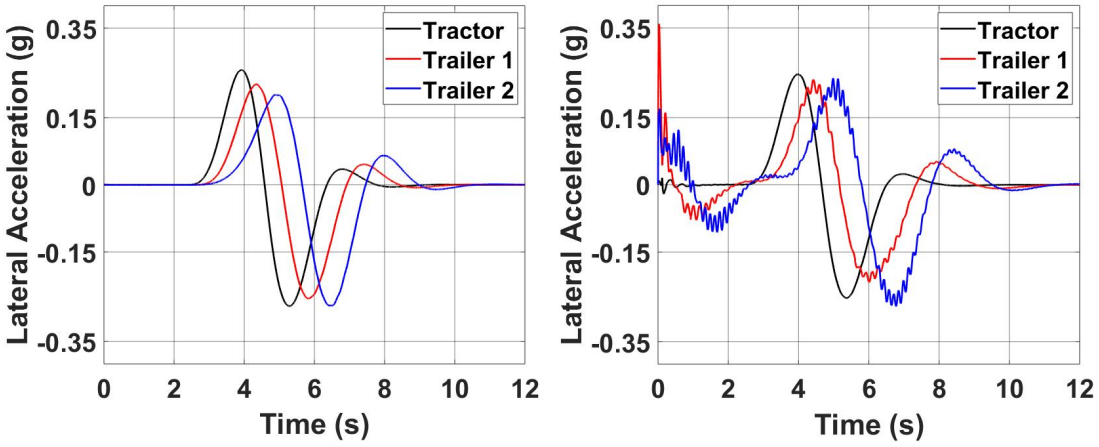

(a) (b)

FIGURE 4.18: Time history of lateral accelerations for the B-Train Double derived from (a) the numerical simulations, and (b) HIL-RT simulations.

As seen in Figure 4.18, similar lateral acceleration responses of the vehicle based on the HIL-RT and numerical simulations are observed. The lateral acceleration peaks show agreement between the numerical and HIL-RT simulations. The RWA ratios determined using the numerical and HIL-RT simulations are 0.9959 and 1.0724, respectively. The relative error of the RWA measures derived from the two simulations is 7.68%. The error between the two simulation methods may be attributed to the noise generated from the angular sensor. The sensor noise is shown in Figure 4.18 (b).

Table 4.4 lists the RWA measures at the specified trailers payload achieved using the two simulation methods. As seen in Table 4.4, the maximum error occurs when the payload is 26,000 kg. The relatively large error may be due to the dynamic lateral load transfer at high payloads [24]. Moreover, RWA measures derived from the numerical simulations show a distinct tendency to increase with the increase of the trailers payload. However, the results based on the HIL-RT simulations show different behaviour. The leading cause could be associated with sensor noises. As shown in Figure 4.18 (b), the sensor noise ripples occur around the peaks of the lateral acceleration curves of the trailers. These ripples could thoroughly affect the RWA measures. Overall, excellent agreement is achieved between the results derived from the two simulation methods.

TABLE 4.4: The RWA measures of the B-Train Double with robust controller derived from HIL-RT and numerical simulations (NS) under the closed-loop SLC maneuver.

Case No.	Weight (kg)	RWA		Error %
		HIL	NS	
1	0	1.0724	0.9959	7.68%
2	10,000	1.0135	1.0354	2.11%
3	15,000	0.9867	1.0567	6.62%
4	26,000	0.9376	1.0622	11.73%

Figure 4.18 shows only the lateral acceleration responses of the B-Train Double with the robust ATS system obtained from the numerical and HIL-RT simulations, under the closed-loop SLC maneuver with trailers payload of 0.0 kg.

The respective lateral acceleration responses at other trailers payloads listed in Table 4.4 are offered in Appendix A.4.

4.5 Summary

In this chapter, the robustness of the LQR- and LMI+LQR-based controllers are tested in three scenarios. The three scenarios are specified as 1) under the condition of varying trailers' payloads and absence of ATS ATC, the dynamics of the baseline vehicle without ATS is compared with those of the vehicle with the LQR- and LMI+LQR-based controller, 2) under the condition of varying trailers' payloads and constant ATS ATC, the performance of the LQR-based controller is compared with that of the LMI+LQR-based controller, and 3) under the condition of constant trailer's payload and varying ATS ATC, the performance of the LQR-based controller is compared with that of the LMI+LQR-based controller. Simulation results indicate that the RWA ratio increases with the increase of either the trailers payload or the ATS ATC. It is observed that the LMI+LQR-based controller shows a more robust performance compared against the LQR-based controller. Moreover, the LMI+LQR-based controller is tested and validated using both the numerical and HIL-RT simulations.

Chapter 5

Conclusions

5.1 Conclusions

This thesis proposes and evaluates the LQR- and LMI+LQR-based ATS controllers for improving the high-speed lateral stability of a B-Train Double, a commonly used MTAHV in Canada. To design the controllers, a linear 4-DOF yaw-plane model is derived to represent the B-Train Double, and the linear model is validated with a nonlinear yaw-roll model developed in TruckSim. The robustness of the proposed controllers is evaluated subject two uncertain parameters, i.e., trailers payload and ATC. The simulation results reveal that both controllers improve the lateral stability of the B-Train Double when compared with the baseline vehicle without ATS.

It is observed that the performance of the LQR-based controller is degraded when the vehicle is subjected to a long ATC. On the other hand, the LMI+LQR-based controller shows robust performance in maintaining good high-speed lateral stability and achieving satisfactory PFOT capability when the vehicle

is subjected to the uncertainties of trailers payload and the ATC. The robustness of the LMI+LQR-based controller is tested and validated using both the numerical and HIL-RT simulations.

The following insightful findings are derived from the research: 1) increasing either the trailers payload or the ATC results in an increase in the RWA ratio, and 2) the trailers payload variation imposes a slighter impact on the RWA ratio compared against the ATC.

5.2 Recommendations for Future Studies

To further improve the proposed robust controller, here are some recommendations to be considered for future research in this area:

1) The versatility of the controller can be evaluated using DHIL, which takes into account the driver's unexpected behaviour.

2) Improving the HIL test bed could lead to better results and reduction in the error difference between numerical and HIL-RT simulations.

3) Field testing with an experimental vehicle can be applied to examine the feasibility of the ATS controller design.

List of Publications

1. **Author:** Mutaz Keldani and Yuping He. Design Analysis of an Active Trailer Steering System for Multi-Trailer Articulated Heavy Vehicles. CSME International Congress, 2019. (In Press)

2. **Author:** Mutaz Keldani and Yuping He. Design of an Improved Robust Active Trailer Steering Controller for a Multi-Trailer Articulated Heavy Vehicle Using Software/Hardware-in-the-Loop Real-Time Simulations. IAVSD, 2019. (Submitted)

3. **Author:** Mutaz Keldani, Khizar Qureshi, Yuping He, and Ramiro Liscano. Design and Optimization of a Robust Active Trailer Steering System for Car-Trailer Combinations. No. 2019-01-0433. SAE Technical Paper, 2019.

4. **Author:** Mutaz Keldani and Yuping He. Design of Electronic Stability Control (ESC) Systems for Car-trailer Combinations. EasyChair Preprint no. 313, Easy-Chair, 2018.

5. **Co-Author:** Huiyong Zhao, Baohua Wang, Guangde Zhang, and Mutaz Keldani. Comparison of Different Steering Ratios on Steering by Wire Vehicle. CSME International Congress, 2019. (In Press)

References

[1] Angela Jannini Weissmann, Jose Weissmann, Athanassios Papagiannakis, and Jaya Lakshmi Kunisetty. Potential impacts of longer and heavier vehicles on texas pavements. *Journal of Transportation Engineering*, 139(1): 75–80, 2012.

[2] MTO. Long combination vehicle (LCV) program. `http://www.mto.gov.on.ca/english/trucks/long-combination-vehicles.shtml`, February 2017.

[3] Md Islam. *Parallel design optimization of multi-trailer articulated heavy vehicles with active safety systems*. PhD thesis, University of Ontario Institute of Technology, 2013.

[4] Aivis Grislis. Longer combination vehicles and road safety. *Transport*, 25 (3):336–343, 2010.

[5] Tushita Sikder. Design of active trailer steering systems for long combination vehicles using robust control techniques. Master's thesis, University of Ontario Institute of Technology, 2017.

[6] Jesse Brown. High-speed lateral stability analysis of articulated heavy vehicles using driver-in-the-loop real time simulation. Master's thesis, University of Ontario Institute of Technology, 2018.

[7] Yuping He, Md Manjurul Islam, Shenjin Zhu, and Thomas Hu. A design synthesis framework for directional performance optimization of multi-trailer articulated heavy vehicles with trailer lateral dynamic control systems. *Proceedings of the Institution of Mechanical Engineers, Part D: Journal of Automobile Engineering*, 231(8):1096–1125, 2017.

[8] Saurabh Kapoor. Fault-tolerant control of active trailer steering systems for multi-trailer articulated heavy vehicles. Master's thesis, University of Ontario Institute of Technology, 2017.

[9] Qiushi Wang. Design and validation of active trailer steering systems for articulated heavy vehicles using driver-hardware-in-the-loop real-time simulation. Master's thesis, University of Ontario Institute of Technology, 2015.

[10] Anne T McCartt, Veronika Shabanova Northrup, and Richard A Retting. Types and characteristics of ramp-related motor vehicle crashes on urban interstate roadways in northern virginia. *Journal of Safety Research*, 35(1): 107–114, 2004.

[11] Xin Gu, Mohamed Abdel-Aty, Qiaojun Xiang, Qing Cai, and Jinghui Yuan. Utilizing uav video data for in-depth analysis of drivers crash risk at interchange merging areas. *Accident Analysis & Prevention*, 123:159–169, 2019.

[12] P Fancher and C Winkler. Directional performance issues in evaluation and design of articulated heavy vehicles. *Vehicle System Dynamics*, 45(7-8):607–647, 2007.

[13] Jonathan D Regehr, Jeannette Montufar, and Garreth Rempel. Safety performance of longer combination vehicles relative to other articulated trucks. *Canadian Journal of Civil Engineering*, 36(1):40–49, 2008.

[14] RD Ervin and Y Guy. Influence of weights and dimensions on the stability and control of heavy trucks in canada-part 2. 1986.

[15] Qiushi Wang and Yuping He. A study on single lane-change manoeuvres for determining rearward amplification of multi-trailer articulated heavy vehicles with active trailer steering systems. *Vehicle System Dynamics*, 54 (1):102123, 2015. doi: 10.1080/00423114.2015.1123280.

[16] Richard L Roebuck, Andrew MC Odhams, and David Cebon. An automatically reconfigurable software-based safety system for rear-steering multi-unit vehicles. *Proceedings of the Institution of Mechanical Engineers, Part D: Journal of automobile engineering*, 229(2):143–162, 2015.

[17] AMC Odhams, RL Roebuck, and C Cebon. Implementation of active steering on a multiple trailer long combination vehicle. *Cambridge University, Engineering Department*, pages 1–13, 2010.

[18] Chen He. Rollover prediction for double trailer articulated heavy vehicles via recurrent neural network. Master's thesis, University of Ontario Institute of Technology, 2016.

[19] Qiushi Wang and Yuping He. Design validation of active trailer steering systems for improving the low-speed manoeuvrability of multi-trailer articulated heavy vehicles using driver-hardware/software-in-the-loop real-time simulations. *International journal of vehicle performance*, 2(1):58–84, 2015.

[20] Zhu Shenjin. *Coordinated control of active safety systems for multi-trailer articulated heavy vehicles*. PhD thesis, University of Ontario Institute of Technology, 2016.

[21] Zhituo Ni. Design and validation of high speed active trailer steering system for articulated heavy vehicle. Master's thesis, University of Ontario Institute of Technology, 2016.

[22] Md Islam. Design synthesis of articulated heavy vehicles with active trailer steering systems. Master's thesis, University of Ontario Institute of Technology, 2010.

[23] Yuping He, Md Manjurul Islam, Shenjin Zhu, and Thomas Hu. A design synthesis framework for directional performance optimization of multi-trailer articulated heavy vehicles with trailer lateral dynamic control systems. *Proceedings of the Institution of Mechanical Engineers, Part D: Journal of Automobile Engineering*, 231(8):10961125, 2016. doi: 10.1177/0954407016671284.

[24] Zhituo Ni and Yuping He. Design and validation of a robust active trailer steering system for multi-trailer articulated heavy vehicles. *Vehicle System Dynamics*, page 127, 2018. doi: 10.1080/00423114.2018.1529322.

[25] Md Manjurul Islam, Yuping He, Shenjin Zhu, and Qiushi Wang. A comparative study of multi-trailer articulated heavy-vehicle models. *Proceedings of the Institution of Mechanical Engineers, Part D: Journal of Automobile Engineering*, 229(9):12001228, 2014. doi: 10.1177/0954407014557053.

[26] Xue Jun Ding and Yu Ping He. Real-time simulations for design of active safety systems for multi-trailer articulated heavy vehicles. In *Digital Manufacturing Automation III*, volume 190 of *Applied Mechanics and Materials*, pages 865–869. Trans Tech Publications, 9 2012. doi: 10.4028/www.scientific.net/AMM.190-191.865.

[27] Xuejun Ding, Steve Mikaric, and Yuping He. Design of an active trailer-steering system for multi-trailer articulated heavy vehicles using real-time simulations. *Proceedings of the Institution of Mechanical Engineers, Part D: Journal of Automobile Engineering*, 227(5):643–655, 2013. doi: 10.1177/0954407012461223. URL https://doi.org/10.1177/0954407012461223.

[28] Johan Wideberg and Erik Dahlberg. A comparative study of legislation and stability measures of heavy articulated vehicles in different regions. *International Journal of Heavy Vehicle Systems*, 16(3):354, 2009. doi: 10.1504/ijhvs.2009.027138.

[29] Tian Jie, Chen Qingyun, Song Zhipeng, Xu Lian, and Li Meiying. Stability analysis and trajectory tracking control of articulated heavy vehicles. In *2015 International Conference on Intelligent Transportation, Big Data and Smart City*, pages 744–748. IEEE, 2015.

[30] Caizhen Cheng, Richard Roebuck, Andrew Odhams, and David Cebon. High-speed optimal steering of a tractor–semitrailer. *Vehicle system dynamics*, 49(4):561–593, 2011.

[31] Peter Sweatman and Brendan Coleman. Productivity opportunities with steerable axles. In *7th International Symposium on Heavy Vehicle Weights & Dimensions Delft, the Netherlands*, 2002.

[32] Caizhen Cheng and David Cebon. Improving roll stability of articulated heavy vehicles using active semi-trailer steering. *Vehicle System Dynamics*, 46(S1):373–388, 2008.

[33] PA LeBlanc, M El-Gindy, and JHF Woodrooffe. Self-steering axles: theory and practice. Technical report, SAE Technical Paper, 1989.

[34] H Prem and K Atley. Performance evaluation of the trackaxle (tm) steerable axle system. In *International Symposium on Heavy Vehicle Weights and Dimensions, 7th, 2002, Delft, The Netherlands*, 2002.

[35] Brian Jujnovich and David Cebon. Comparative performance of semi-trailer steering systems. In *7th International Symposium on Heavy Vehicle Weights & Dimensions, Delft, The Netherlands, Europe*, 2002.

[36] Bin Li and Subhash Rakheja. Yaw stability enhancement of articulated commercial vehicles via gain-scheduling optimal control approach. *SAE International Journal of Commercial Vehicles*, 10(2017-01-0437):275–282, 2017.

[37] PWCE Fancher, C Winkler, R Ervin, and Hongli Zhang. Using braking to control the lateral motions of full trailers. *Vehicle System Dynamics*, 29(S1): 462–478, 1998.

[38] Li Mai, Pu Xie, and Changfu Zong. Research on algorithm of stability control for tractor semi-trailer. In *2009 International Conference on Mechatronics and Automation*, pages 4224–4228. IEEE, 2009.

[39] Scott Kimbrough, Mark Elwell, and Chunchih Chiu. Braking controllers and steering controllers for combination vehicles. *International Journal of Heavy Vehicle Systems*, 1(2):195–223, 1994.

[40] Arnaud JP Miege and David Cebon. Optimal roll control of an articulated vehicle: theory and model validation. *Vehicle system dynamics*, 43(12):867–884, 2005.

[41] SM Shariatmadar, M Manteghi, and M Tajdari. Enhancement of articulated heavy vehicle stability by optimal linear quadratic regulator (lqr) controller of roll-yaw dynamics. 2012.

[42] RC Lin, David Cebon, and DJ Cole. Active roll control of articulated vehicles. *Vehicle System Dynamics*, 26(1):17–43, 1996.

[43] RC Lin, D Cebon, and DJ Cole. Optimal roll control of a single-unit lorry. *Proceedings of the Institution of Mechanical Engineers, Part D: Journal of Automobile Engineering*, 210(1):45–55, 1996.

[44] David JM Sampson and David Cebon. Achievable roll stability of heavy road vehicles. *Proceedings of the Institution of Mechanical Engineers, Part D: Journal of Automobile Engineering*, 217(4):269–287, 2003.

[45] David JM Sampson and David Cebon. Active roll control of single unit heavy road vehicles. *Vehicle System Dynamics*, 40(4):229–270, 2003.

[46] Md Manjurul Islam and Islam He. A parallel design optimisation method for articulated heavy vehicles with active safety systems. *International journal of heavy vehicle systems*, 20(4):327–341, 2013.

[47] Sogol Kharrazi, Mathias Lidberg, and Jonas Fredriksson. A generic controller for improving lateral performance of heavy vehicle combinations. *Proceedings of the Institution of Mechanical Engineers, Part D: Journal of Automobile Engineering*, 227(5):619–642, 2013.

[48] S Kharrazi. Steering based lateral performance control of long heavy vehicle combinations [phd thesis]. *Chalmers University of Technology*, 2012.

[49] Krishna Rangavajhula and H-S Jacob Tsao. Active trailer steering control of an articulated system with a tractor and three full trailers for tractor-track following. *International Journal of Heavy Vehicle Systems*, 14(3):271–293, 2007.

[50] K Rangavajhula and HS J Tsao. Command steering of trailers and command-steering-based optimal control of an articulated system for tractor-track following. *Proceedings of the Institution of Mechanical Engineers, Part D: Journal of Automobile Engineering*, 222(6):935–954, 2008.

[51] AMC Odhams, RL Roebuck, BA Jujnovich, and D Cebon. Active steering of a tractor–semi-trailer. *Proceedings of the Institution of Mechanical Engineers, Part D: Journal of Automobile Engineering*, 225(7):847–869, 2011.

[52] Mohammad Amin Saeedi, Reza Kazemi, and Shahram Azadi. A new robust controller to improve the lateral dynamic of an articulated vehicle carrying liquid. *Proceedings of the Institution of Mechanical Engineers, Part K: Journal of Multi-body Dynamics*, 231(2):295–315, 2017.

[53] AMC Odhams, RL Roebuck, D Cebon, and CB Winkler. Dynamic safety of active trailer steering systems. *Proceedings of the Institution of Mechanical Engineers, Part K: Journal of multi-body dynamics*, 222(4):367–380, 2008.

[54] Sina Milani, Y Samim Ünlüsoy, Hormoz Marzbani, and Reza N Jazar. Semi-trailer steering control for improved articulated vehicle manoeuvrability and stability. *Nonlinear Engineering*, 8(1):568–581, 2019.

[55] Kyong-il Kim, Hsin Guan, Bo Wang, Rui Guo, and Fan Liang. Active steering control strategy for articulated vehicles. *Frontiers of Information Technology & Electronic Engineering*, 17(6):576–586, 2016.

[56] A Percy and I Spark. A numerical control algorithm for a b-double truck–trailer with steerable trailer wheels and active hitch angles. *Proceedings of the Institution of Mechanical Engineers, Part D: Journal of automobile engineering*, 226(3):289–300, 2012.

[57] Deepa S Warrier. Modelling and analysis of active vehicle steering control using nonlinear controller. *International Journal of Advanced Research in Electrical, Electronics and Instrumentation Engineering*, pages 1–11, 2017.

[58] Qiushi Wang, Shenjin Zhu, and Yuping He. Model reference adaptive control for active trailer steering of articulated heavy vehicles. Technical report, SAE Technical Paper, 2015.

[59] Tushita Sikder, Saurabh Kapoor, and Yuping He. Robust control of active trailer steering systems for long combination vehicles. In *Dynamics of Vehicles on Roads and Tracks Vol 1: Proceedings of the 25th International Symposium on Dynamics of Vehicles on Roads and Tracks (IAVSD 2017), 14-18 August 2017, Rockhampton, Queensland, Australia*, page 99. CRC Press, 2017.

[60] Xiujian Yang, Juntao Song, and Jin Gao. Fuzzy logic based control of the lateral stability of tractor semitrailer vehicle. *Mathematical Problems in Engineering*, 2015, 2015.

[61] Filipe Marques Barbosa, Lucas Barbosa Marcos, Maíra Martins da Silva, Marco Henrique Terra, and Valdir Grassi Junior. Robust path-following control for articulated heavy-duty vehicles. *Control Engineering Practice*, 85:246–256, 2019.

[62] Maliheh Sadeghi Kati, Hakan Köroğlu, and Jonas Fredriksson. Robust lateral control of long-combination vehicles under moments of inertia and tyre cornering stiffness uncertainties. *Vehicle System Dynamics*, pages 1–27, 2018.

[63] M Ei-Gindy, N Mrad, and X Tong. Sensitivity of rearward amplication control of a truck/full trailer to tyre cornering stiffness variations. *Proceedings*

of the Institution of Mechanical Engineers, Part D: Journal of Automobile Engineering, 215(5):579–588, 2001.

[64] Moustapha Doumiati, Ali Charara, Alessandro Victorino, and Daniel Lechner. *Vehicle dynamics estimation using Kalman filtering: experimental validation*. John Wiley & Sons, 2012.

[65] Caizhen Cheng and David Cebon. Parameter and state estimation for articulated heavy vehicles. *Vehicle System Dynamics*, 49(1-2):399–418, 2011.

[66] BA Jujnovich and D Cebon. Path-following steering control for articulated vehicles. *Journal of Dynamic Systems, Measurement, and Control*, 135(3): 031006, 2013.

[67] Nobuo Hata, Shunichi Hasegawa, Ken Ito, Takeshi Fujishiro, et al. A control method for 4ws truck to suppress excursion of a body rear overhang. Technical report, SAE Technical Paper, 1989.

[68] Ikurou Notsu, Sadahiro Takahashi, and Yoshito Watanabe. Investigation into turning behavior of semi-trailer with additional trailer-wheel steering–a control method for trailer-wheel steering to minimize trailer rear-overhang swing in short turns. Technical report, SAE Technical Paper, 1991.

[69] Marco H Terra, João P Cerri, and João Y Ishihara. Optimal robust linear quadratic regulator for systems subject to uncertainties. *IEEE Transactions on Automatic Control*, 59(9):2586–2591, 2014.

[70] Naser Elmi, Abdolreza Ohadi, and Behzad Samadi. Active front-steering control of a sport utility vehicle using a robust linear quadratic regulator method, with emphasis on the roll dynamics. *Proceedings of the Institution of Mechanical Engineers, Part D: Journal of automobile engineering*, 227(12): 1636–1649, 2013.

[71] M Sever, EE Kaya, MS Arslan, and H Yazici. Active trailer braking system design with linear matrix inequalities based multi-objective robust lqr controller for vehicle-trailer systems. In *2016 IEEE Intelligent Vehicles Symposium (IV)*, pages 796–801. IEEE, 2016.

[72] Yuping He and Qiushi Wang. Driver-hardware/software-in-the-loop real-time simulations for the design of active trailer steering systems of multi-trailer articulated heavy vehicles. In *Proceedings of the 12th International Symposium on Advanced Vehicle Control*, pages 22–26, 2014.

[73] Bilin Aksun Guvenc, Levent Guvenc, and Sertaç Karaman. Robust yaw stability controller design and hardware-in-the-loop testing for a road vehicle. *IEEE Transactions on Vehicular Technology*, 58(2):555–571, 2009.

[74] Guo-Dong Yin, Nan Chen, Jin-Xiang Wang, and Ling-Yao Wu. A study on μ-synthesis control for four-wheel steering system to enhance vehicle lateral stability. *Journal of dynamic systems, measurement, and control*, 133 (1):011002, 2011.

[75] Xuejun Ding and Yuping He. Real-time simulations for design of active safety systems for multi-trailer articulated heavy vehicles. In *Applied Mechanics and Materials*, volume 190, pages 865–869. Trans Tech Publ, 2012.

[76] Eungkil Lee. Design optimization of active trailer differential braking systems for car-trailer combinations. Master's thesis, University of Ontario Institute of Technology, 2016.

[77] Truck, Bus Powertrain Steering Committee, et al. A test for evaluating the rearward amplification of multiarticulated vehicles. *SAE Standard J*, 2179, 1993.

[78] John Woodrooffe and L Ash. Long combination vehicle (lcv) safety performance in alberta 1995 to 1998. *Woodrooffe & Associates*, 2001.

[79] Pierre Apkarian and Hoang Duong Tuan. Parameterized lmis in control theory. *SIAM journal on control and optimization*, 38(4):1241–1264, 2000.

[80] Da-Wei Gu, Petko Petkov, and Mihail M Konstantinov. *Robust control design with MATLAB®*. Springer Science & Business Media, 2013.

[81] Jun Li, WeiWei Li, XingWang Hu, WenChuan Sun, and Gang Kong. Pfc performance improvement of ultra-supercritical secondary reheat unit. In *E3S Web of Conferences*, volume 38, page 01002. EDP Sciences, 2018.

[82] ISO ISO14791. Road vehicles-heavy commercial vehicle combinations and articulated buses-lateral stability test methods. Technical report, Tech. rep, 2002.

Appendix A

Appendix A

Table A.1: B-train Double Configuration Distances.

Symbol	Description	Units
	Distances	
D_1	Distance from the front axle to the CG of the tractor	m
D_2	Distance from the CG to the second axle of the tractor	m
D_3	Distance from the CG to the third axle of the tractor	m
D_4	Distance from the CG to the first axle of the first trailer	m
D_5	Distance from the CG to the second axle of the first trailer	m
D_6	Distance from the CG to the third axle of the first trailer	m
D_7	Distance from the CG to the first axle of the second trailer	m
D_8	Distance from the CG to the second axle of the second trailer	m
D_9	Distance from the CG to the third axle of the second trailer	m
h_1	Distance from the CG to the fifth wheel of the tractor	m
h_2	Distance from the tractor's fifth wheel to the CG of the first trailer	m
h_3	Distance from the CG to the fifth wheel of the first trailer	m
h_4	Distance from the first trailer's fifth wheel to the CG of the second trailer	m

Table A.2: B-train Double Configuration Parameters.

Symbol	Description	Units
	Tractor	
m_1	Total mass of tractor	kg
I_1	Yaw moment of inertia of the tractor	kg*mˆ2
$\dot{\gamma}_1$	Yaw rate of the tractor	deg/s
V_{y1}	Lateral velocity of the tractor	m/s
F_{yi}, i=1-3	Lateral force of the tractors 1^{st} to 3^{rd} axles	N
C_i, i=1-3	Cornering stiffness of the tractors 1^{st} to 3^{rd} axles	N/deg
α_i, i=1-3	Side-slip angles of the tractor's 1^{st} to 3^{rd} axles	deg
V_x	Forward velocity	m/s

Symbol	Description	Units
	Trailer 1	
m_2	Total mass of the 1^{st} trailer	kg
I_2	Yaw moment of inertia of the first trailer	kg*mˆ2
$\dot{\gamma}_2$	Yaw rate of the first trailer	deg/s
V_{y2}	Lateral velocity of the first trailer	m/s
F_{yi}, i=4-6	Lateral force of the first trailer's 4^{th} to 6^{th} axles	N
C_i, i=4-6	Cornering stiffness of the first trailer's 4^{th} to 6^{th} axles	N/deg
α_i, i=4-6	Side-slip angles of the first trailer's 4^{th} to 6^{th} axles	deg
V_x	Forward velocity	m/s

Symbol	Description	Units
	Trailer 2	
m_3	Total mass of the 2^{nd} trailer	kg
I_3	Yaw moment of inertia of the second trailer	kg*mˆ2
$\dot{\gamma}_3$	Yaw rate of the second trailer	deg/s
V_{y3}	Lateral velocity of the second trailer	m/s
F_{yi}, i=7-9	Lateral force of the second trailer's 7^{th} to 9^{th} axles	N
C_i, i=7-9	Cornering stiffness of the second trailer's 7^{th} to 9^{th} axles	N/deg
α_i, i=7-9	Side-slip angles of the second trailer's 7^{th} to 9^{th} axles	deg
V_x	Forward velocity	m/s

A.1 Results Achieved Under First Scenario

Table 4.1 - Case No. 2

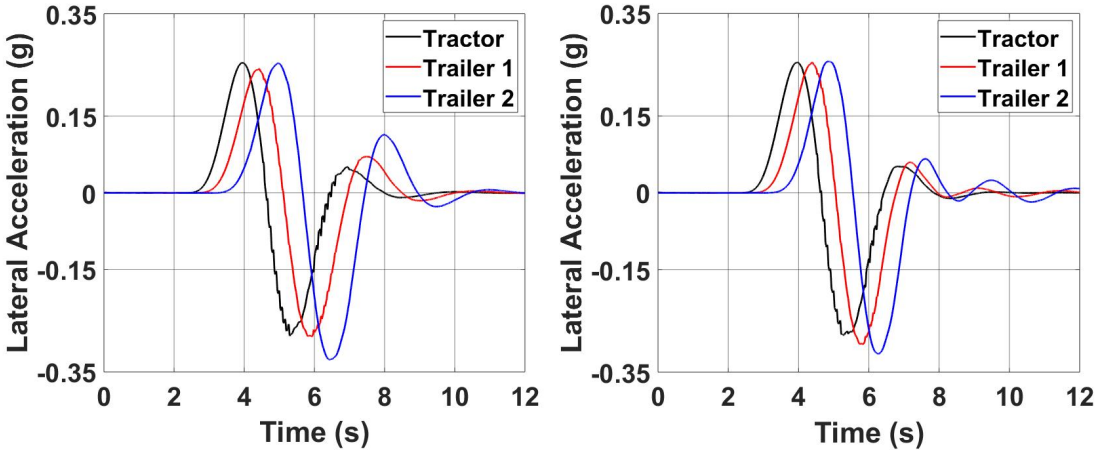

(a) (b)

FIGURE A.1: Time histories of lateral acceleration for the B-train (a) without ATS, and (b) LQR-based ATS controller.

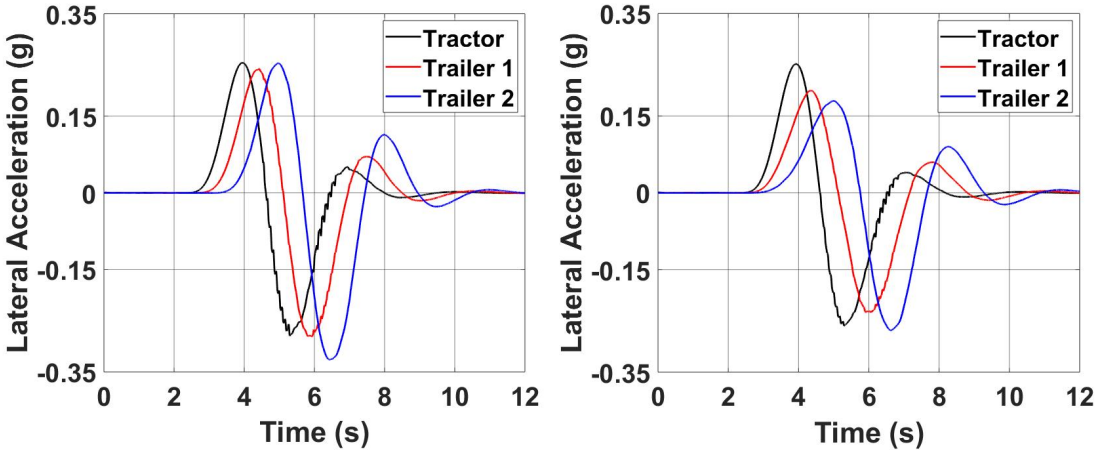

(a) (b)

FIGURE A.2: Time histories of lateral acceleration for the B-train (a) without ATS, and (b) LMI+LQR-based controller.

Table 4.1 - Case No. 3

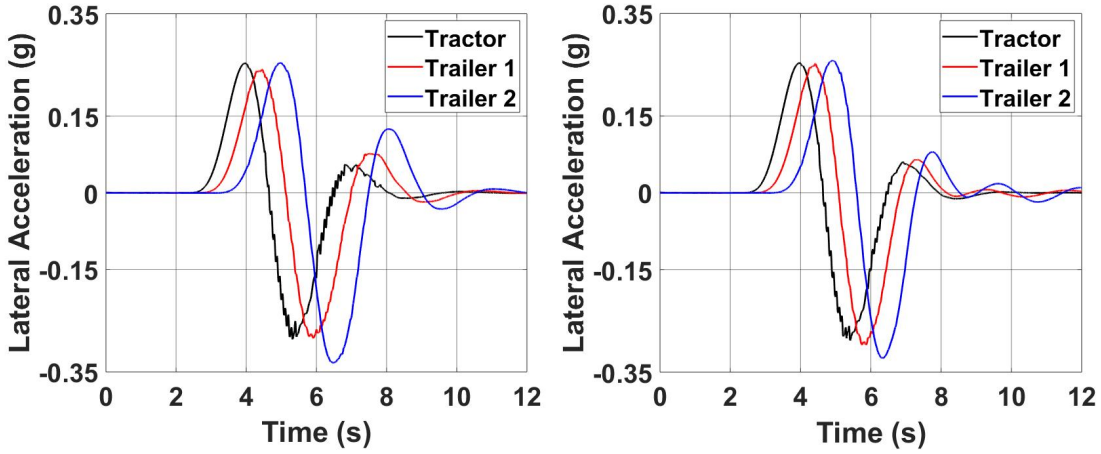

(a) (b)

FIGURE A.3: Time histories of lateral acceleration for the B-train (a) without ATS, and (b) LQR-based ATS controller.

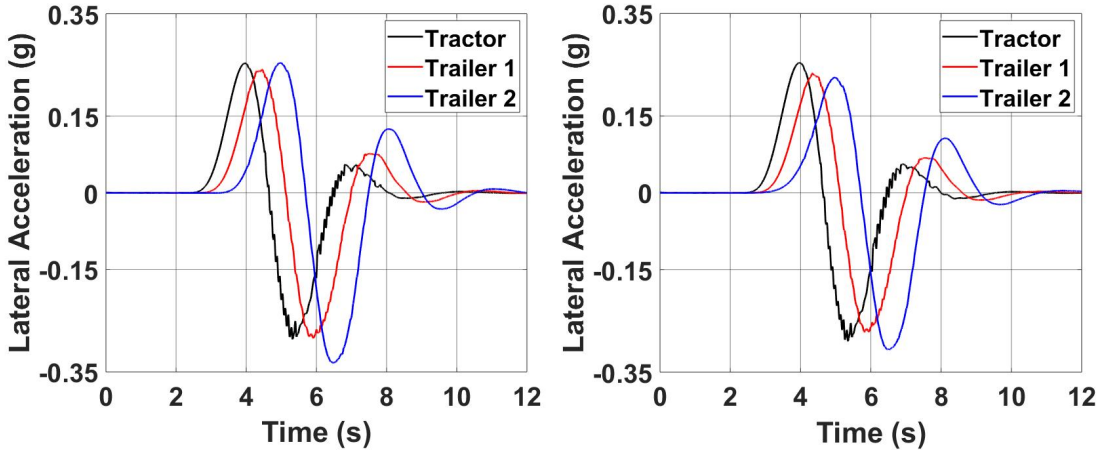

(a) (b)

FIGURE A.4: Time histories of lateral acceleration for the B-train (a) without ATS, and (b) LMI+LQR-based controller.

Table 4.1 - Case No. 4

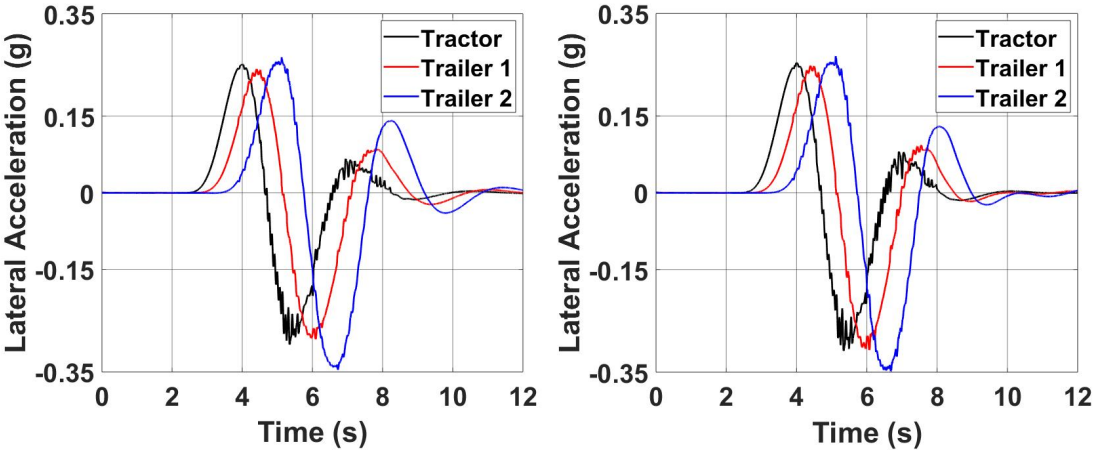

(a) (b)

FIGURE A.5: Time histories of lateral acceleration for the B-train (a) without ATS, and (b) LQR-based ATS controller.

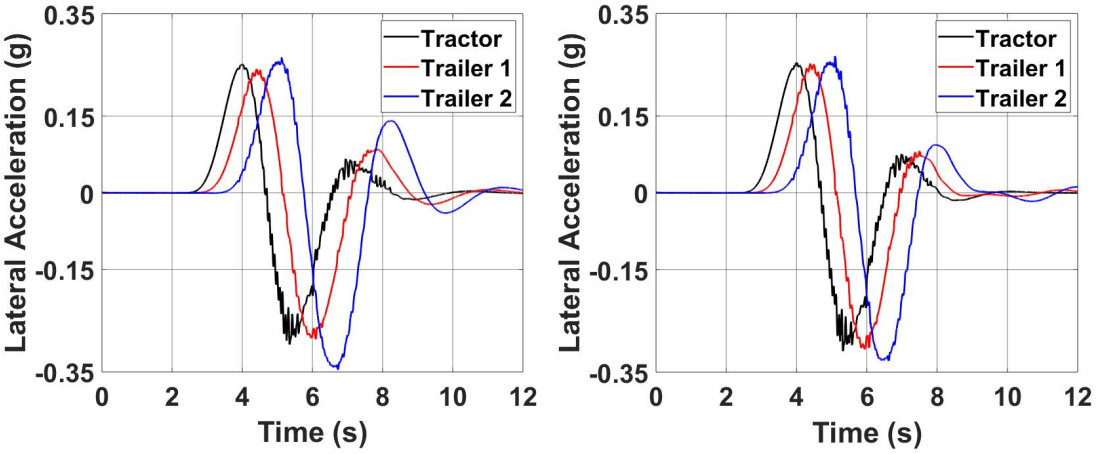

(a) (b)

FIGURE A.6: Time histories of lateral acceleration for the B-train (a) without ATS, and (b) LMI+LQR-based controller.

A.2 Results Achieved Under Second Scenario

Table 4.2 - Case A.1

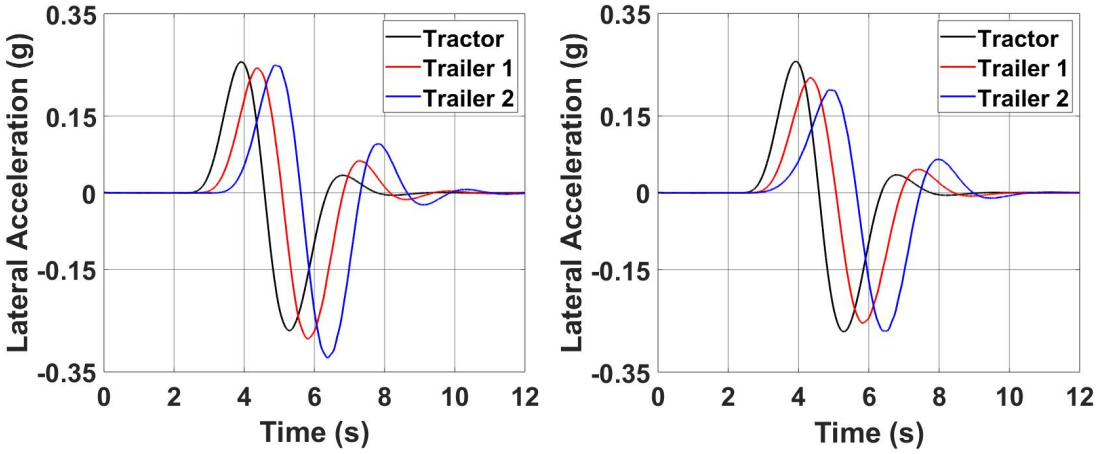

(a) (b)

FIGURE A.7: Time histories of lateral acceleration for the B-train (a) LQR-based ATS controller, and (b) LMI+LQR-based controller.

Table 4.2 - Case A.2

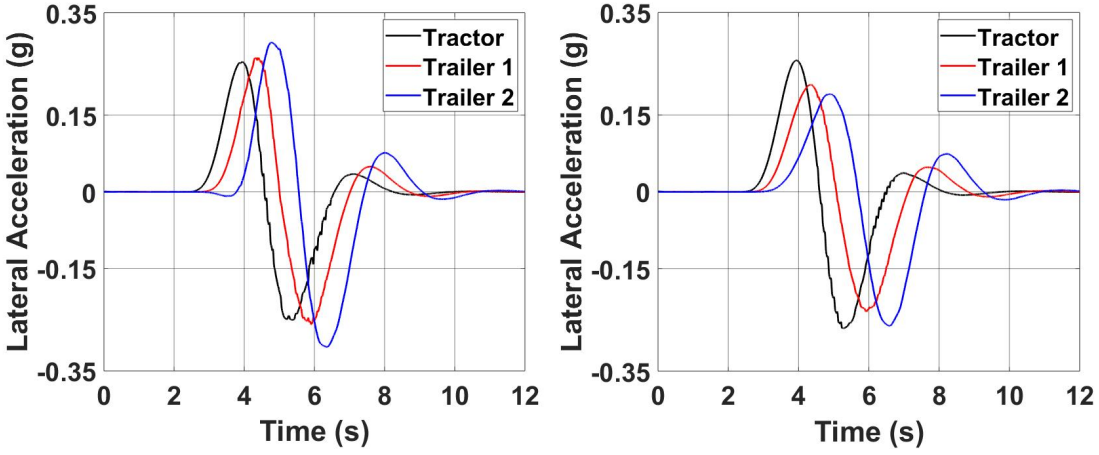

(a) (b)

FIGURE A.8: Time histories of lateral acceleration for the B-train (a) LQR-based ATS controller, and (b) LMI+LQR-based controller.

Table 4.2 - Case A.3

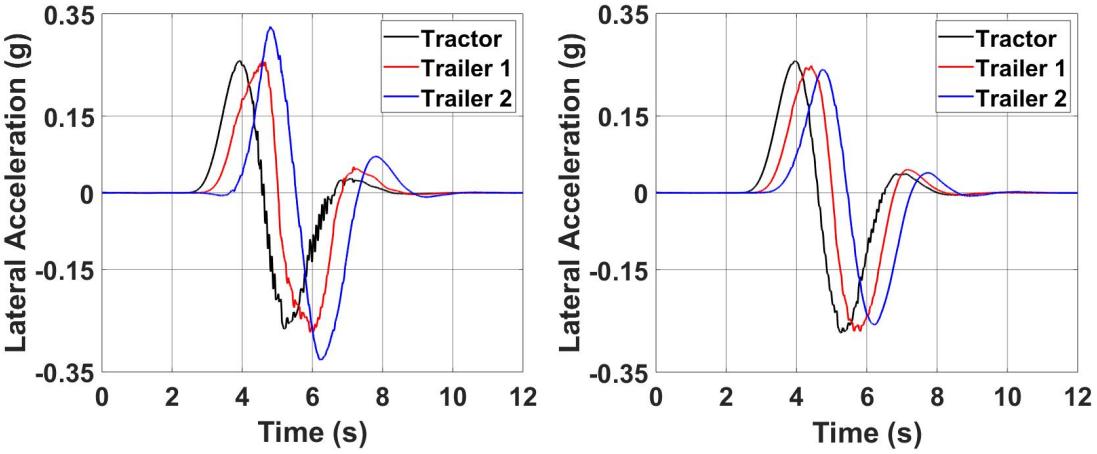

(a) (b)

FIGURE A.9: Time histories of lateral acceleration for the B-train (a) LQR-based ATS controller, and (b) LMI+LQR-based controller.

Table 4.2 - Case A.4

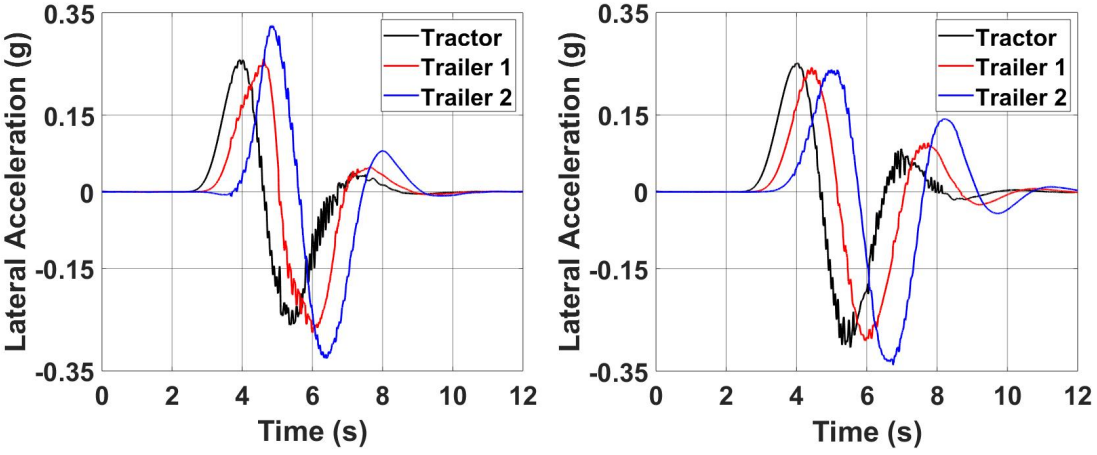

(a) (b)

FIGURE A.10: Time histories of lateral acceleration for the B-train (a) LQR-based ATS controller, and (b) LMI+LQR-based controller.

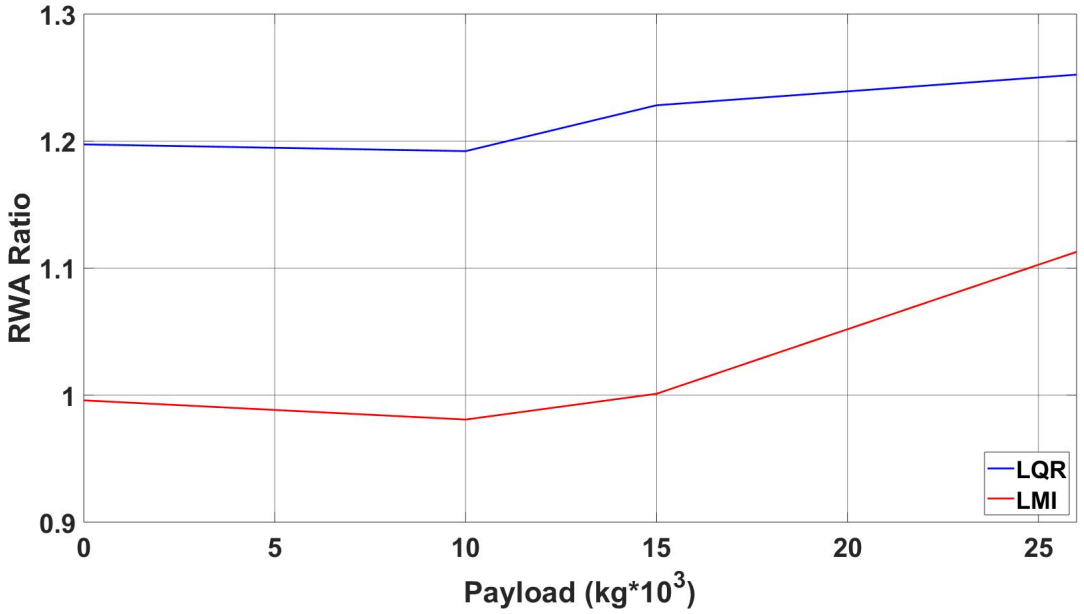

FIGURE A.11: Case A - RWA measure under constant ATC of 0.5 seconds and variation of trailer payload.

Table 4.2 - Case B.1

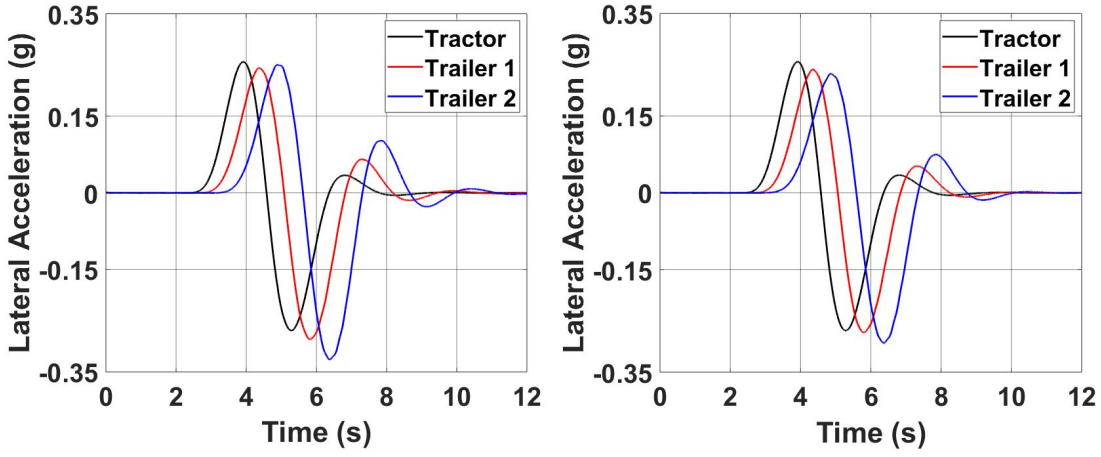

FIGURE A.12: Time histories of lateral acceleration for the B-train (a) LQR-based ATS controller, and (b) LMI+LQR-based controller.

Table 4.2 - Case B.3

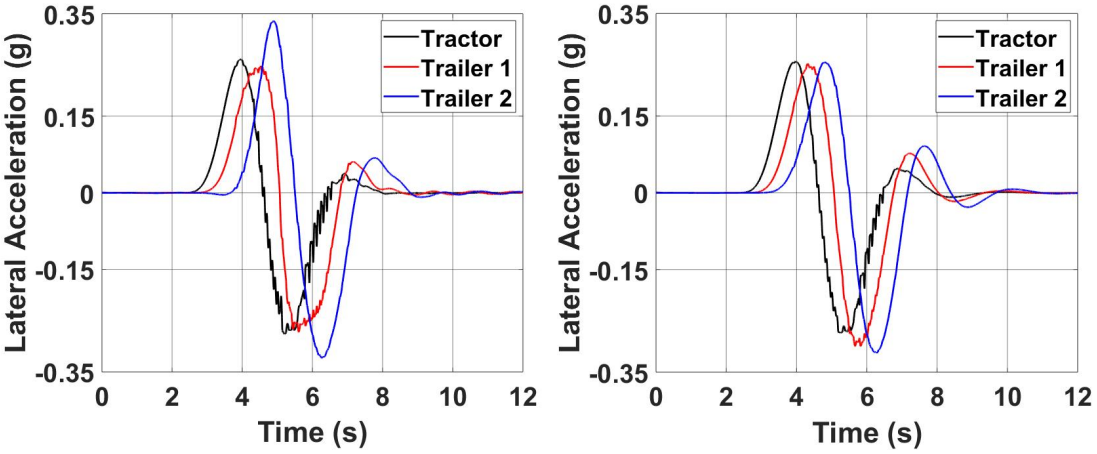

(a) (b)

FIGURE A.13: Time histories of lateral acceleration for the B-train (a) LQR-based ATS controller, and (b) LMI+LQR-based controller.

Table 4.2 - Case B.4

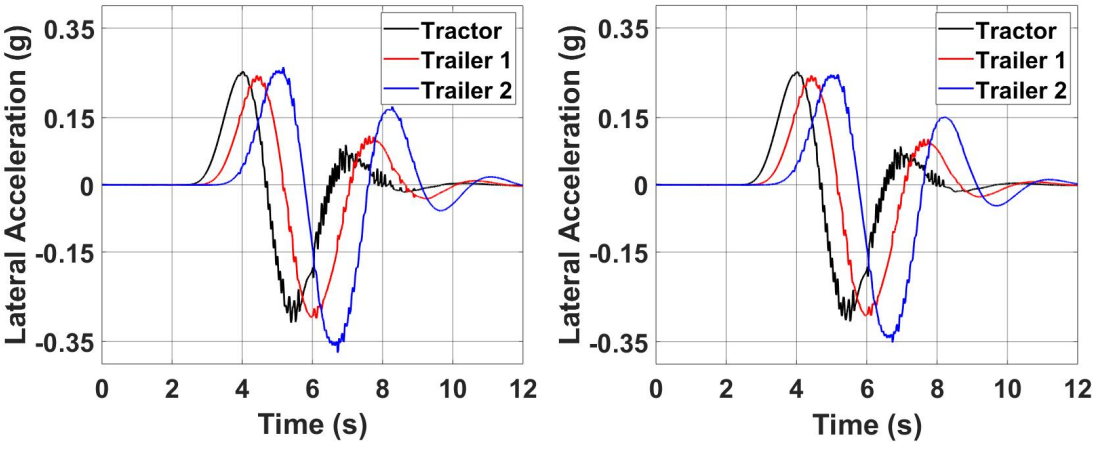

(a) (b)

FIGURE A.14: Time histories of lateral acceleration for the B-train (a) LQR-based ATS controller, and (b) LMI+LQR-based controller.

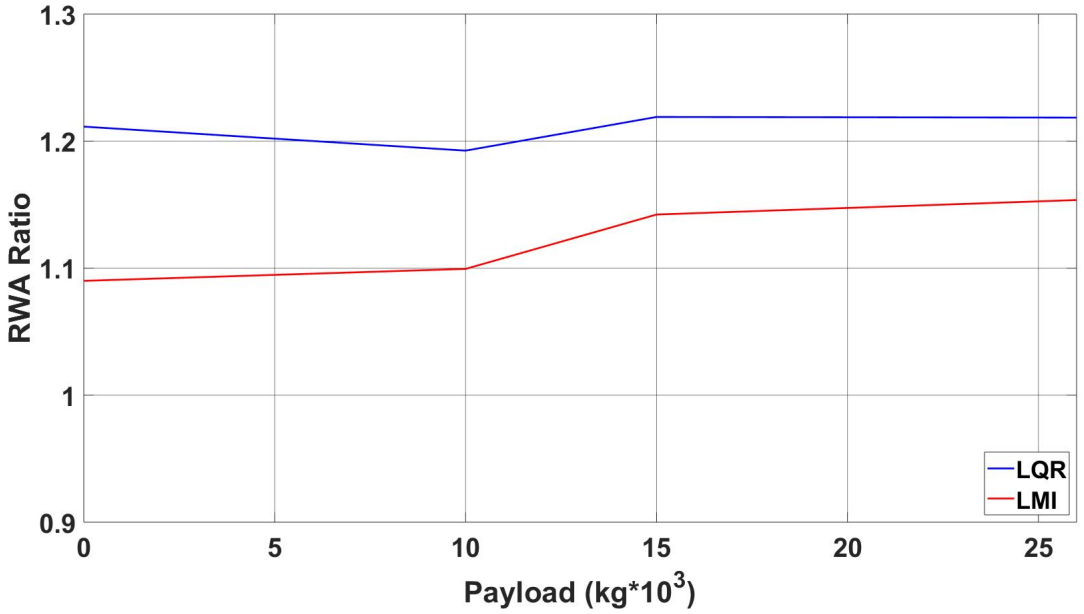

FIGURE A.15: Case B - RWA measure under constant ATC of 1 seconds and variation of trailer payload.

Table 4.2 - Case C.1

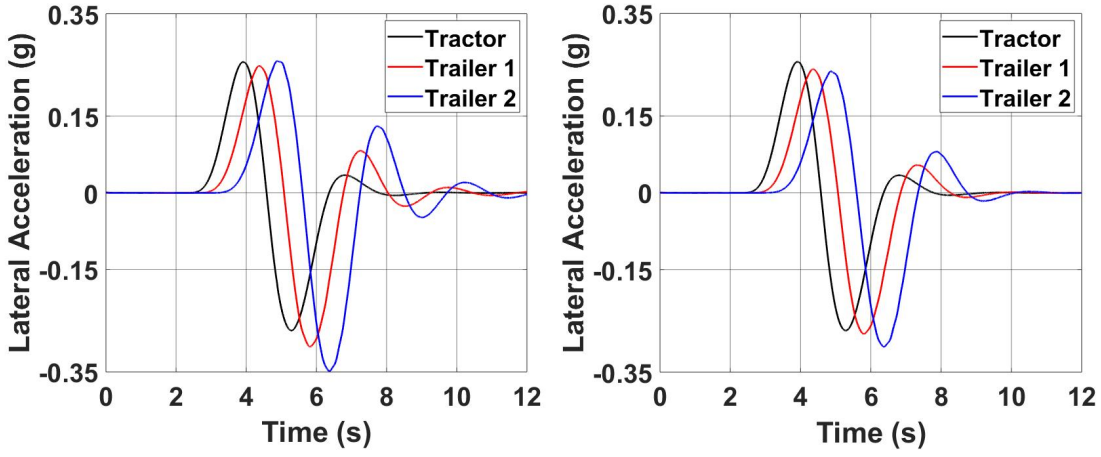

(a) (b)

FIGURE A.16: Time histories of lateral acceleration for the B-train (a) LQR-based ATS controller, and (b) LMI+LQR-based controller.

Table 4.2 - Case C.2

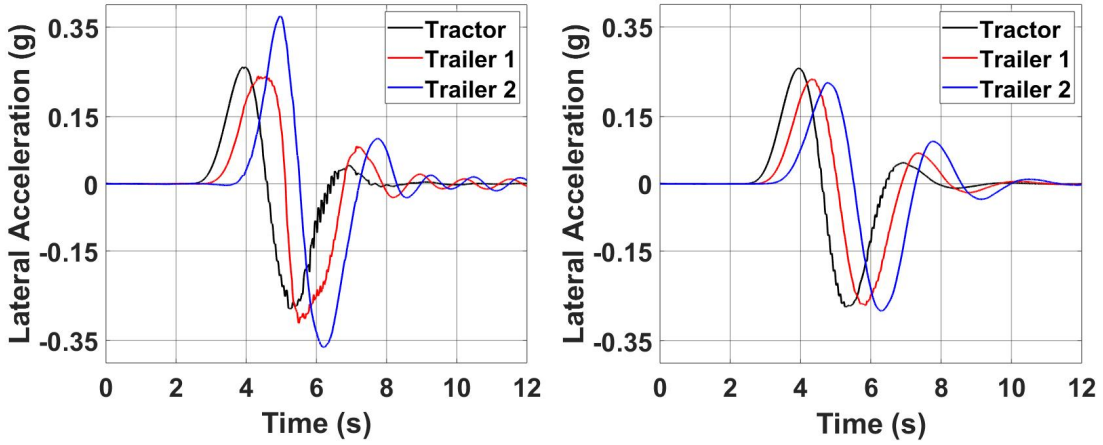

FIGURE A.17: Time histories of lateral acceleration for the B-train (a) LQR-based ATS controller, and (b) LMI+LQR-based controller.

Table 4.2 - Case C.3

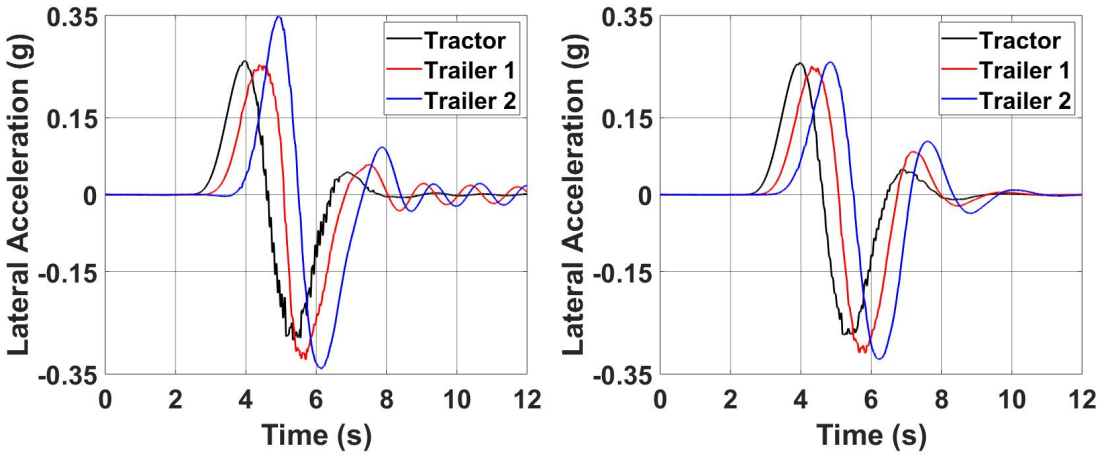

FIGURE A.18: Time histories of lateral acceleration for the B-train (a) LQR-based ATS controller, and (b) LMI+LQR-based controller.

Table 4.2 - Case C.4

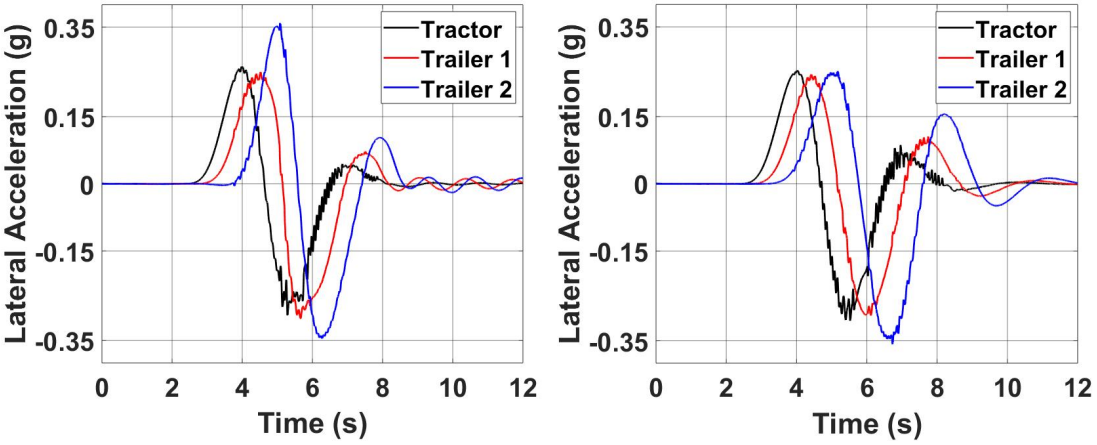

(a) (b)

FIGURE A.19: Time histories of lateral acceleration for the B-train (a) LQR-based ATS controller, and (b) LMI+LQR-based controller.

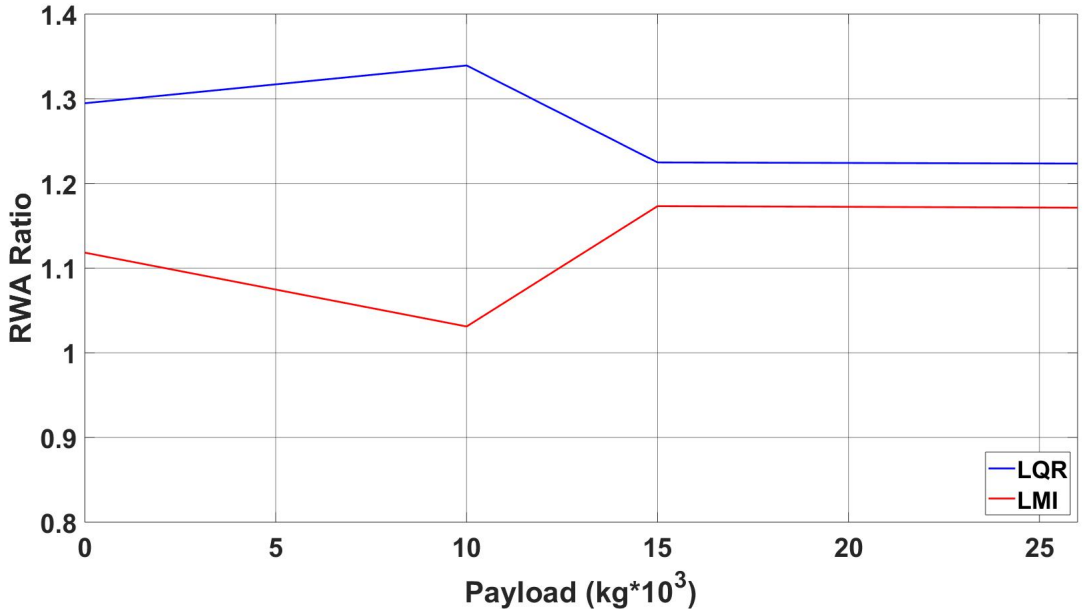

FIGURE A.20: Case C - RWA measure under constant ATC of 1.5 seconds and variation of trailer payload.

Table 4.2 - Case D.1

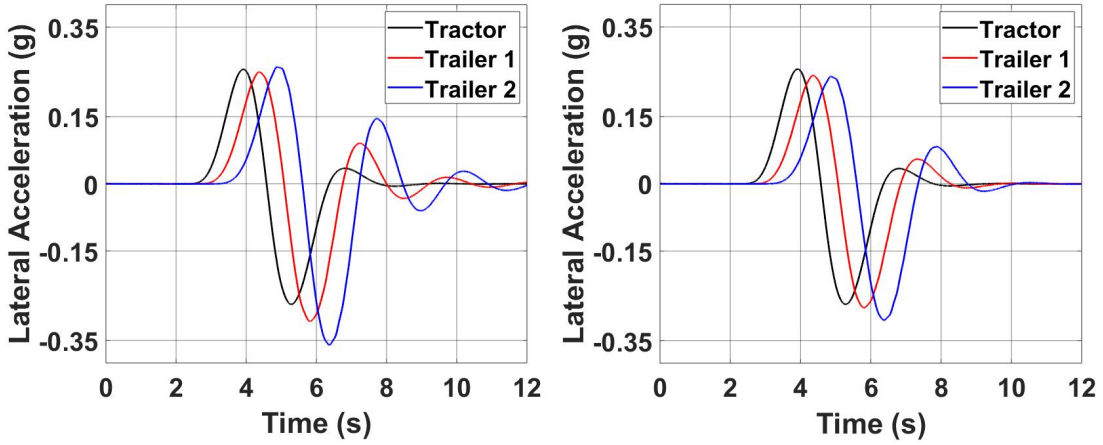

(a) (b)

FIGURE A.21: Time histories of lateral acceleration for the B-train (a) LQR-based ATS controller, and (b) LMI+LQR-based controller.

Table 4.2 - Case D.2

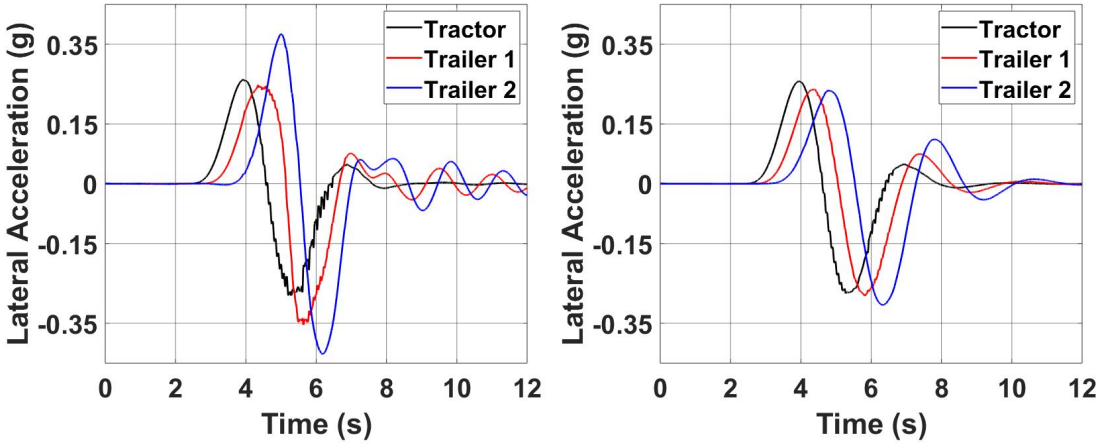

(a) (b)

FIGURE A.22: Time histories of lateral acceleration for the B-train (a) LQR-based ATS controller, and (b) LMI+LQR-based controller.

Table 4.2 - Case D.3

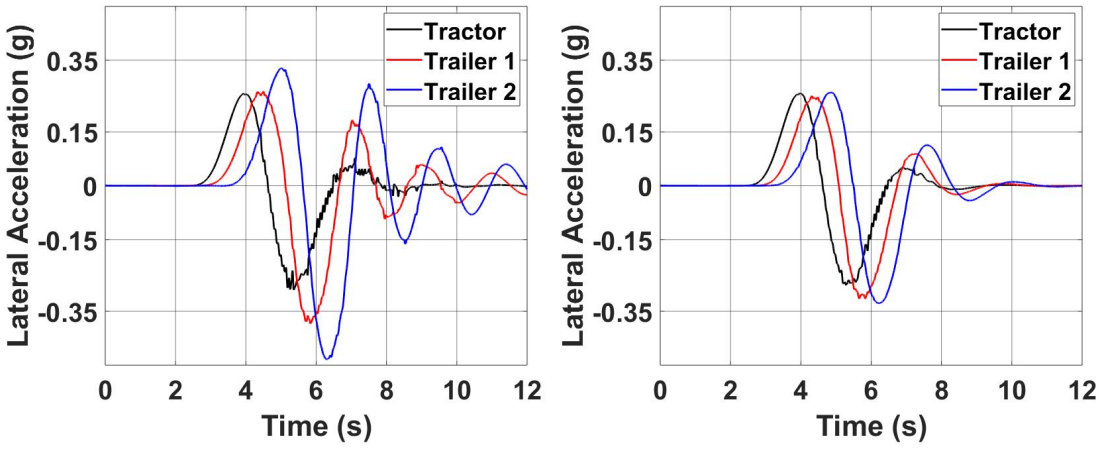

(a) (b)

FIGURE A.23: Time histories of lateral acceleration for the B-train (a) LQR-based ATS controller, and (b) LMI+LQR-based controller.

Table 4.2 - Case D.4

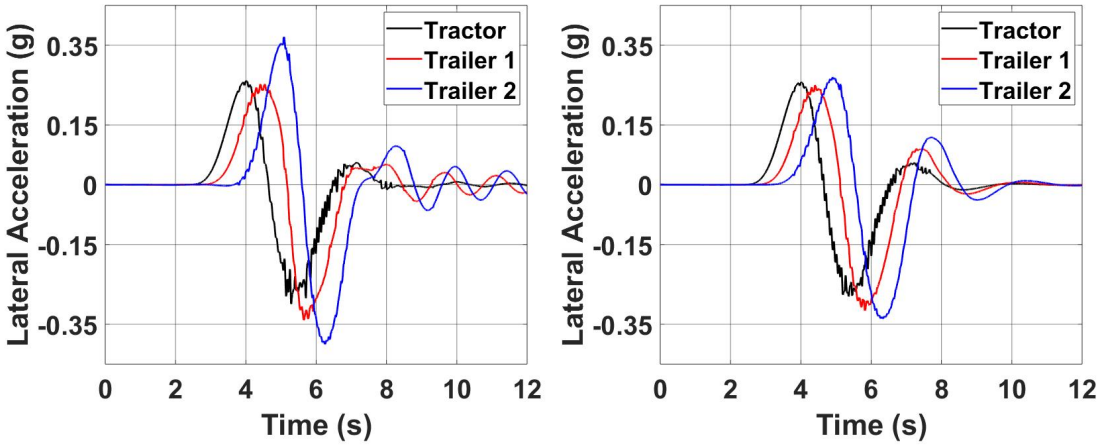

(a) (b)

FIGURE A.24: Time histories of lateral acceleration for the B-train (a) LQR-based ATS controller, and (b) LMI+LQR-based controller.

A.3 Results Achieved Under Third Scenario

Table 4.3 - Case A

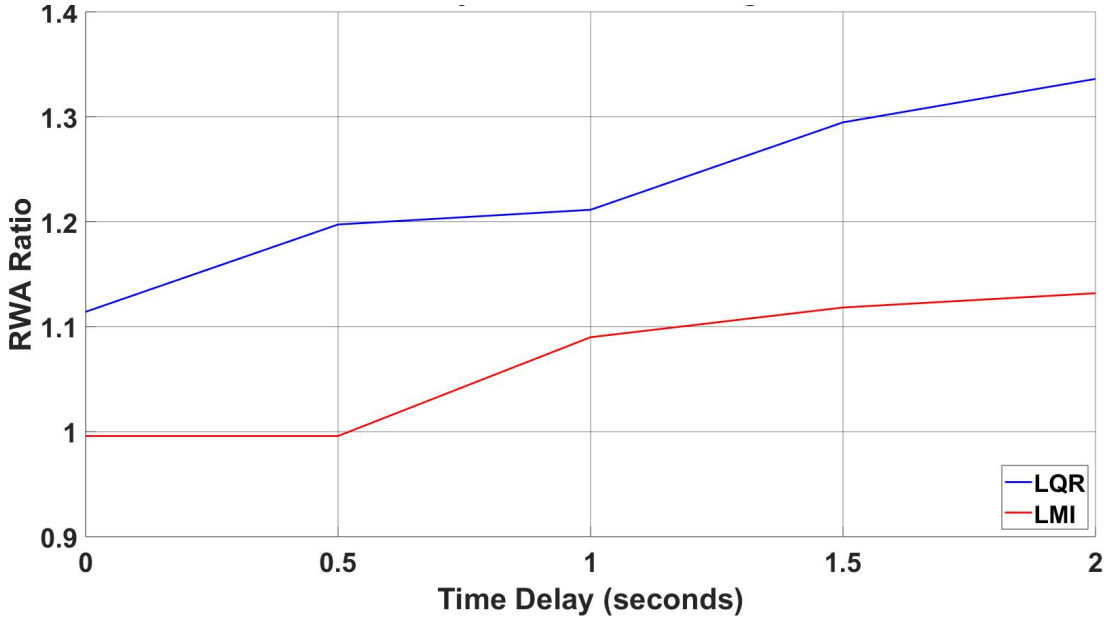

FIGURE A.25: Case A - RWA measure under constant payload of 0 kg and variation of ATC.

Table 4.3 - Case B

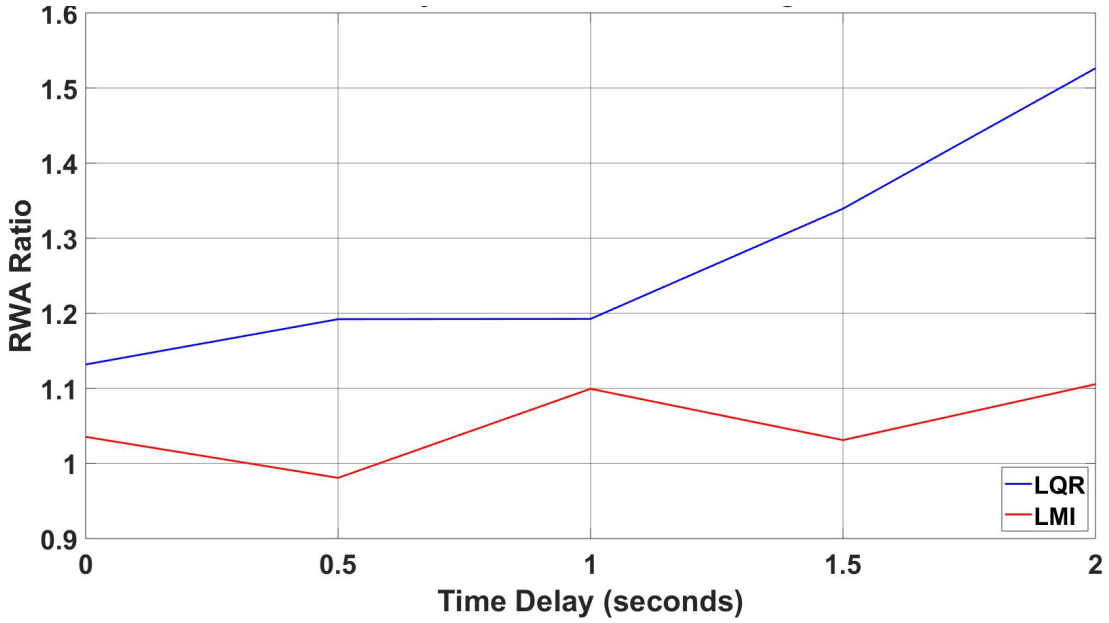

FIGURE A.26: Case B - RWA measure under constant payload of 10,000 kg and variation of ATC.

Table 4.3 - Case C

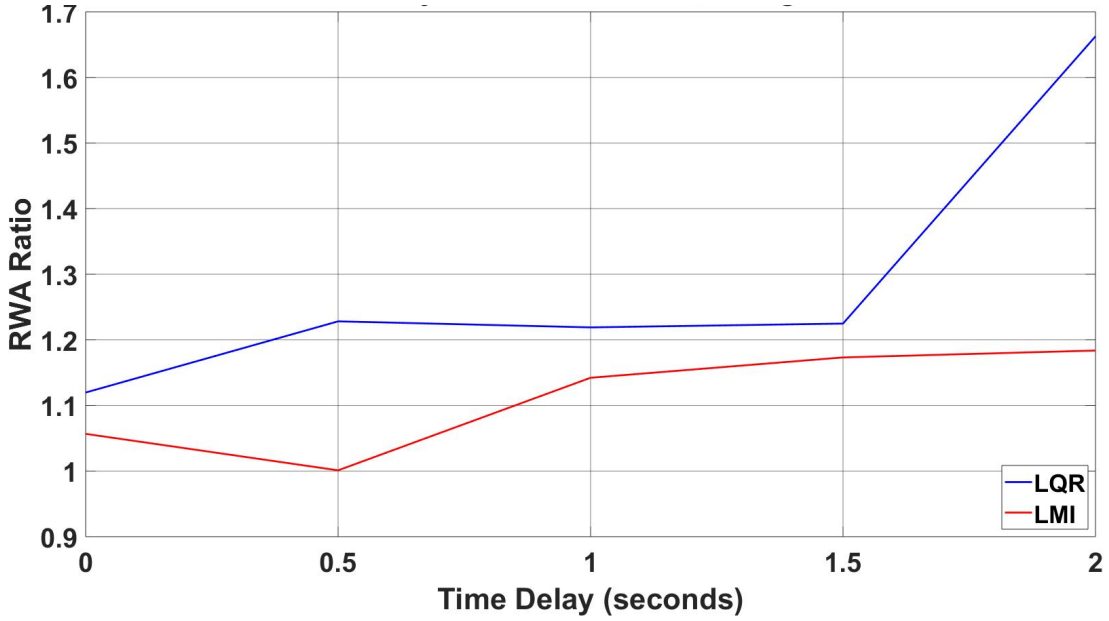

FIGURE A.27: Case C - RWA measure under constant payload of 15,000 kg and variation of ATC.

A.4 Robust Controller Performance Validation

Table 4.4 - Case No. 2

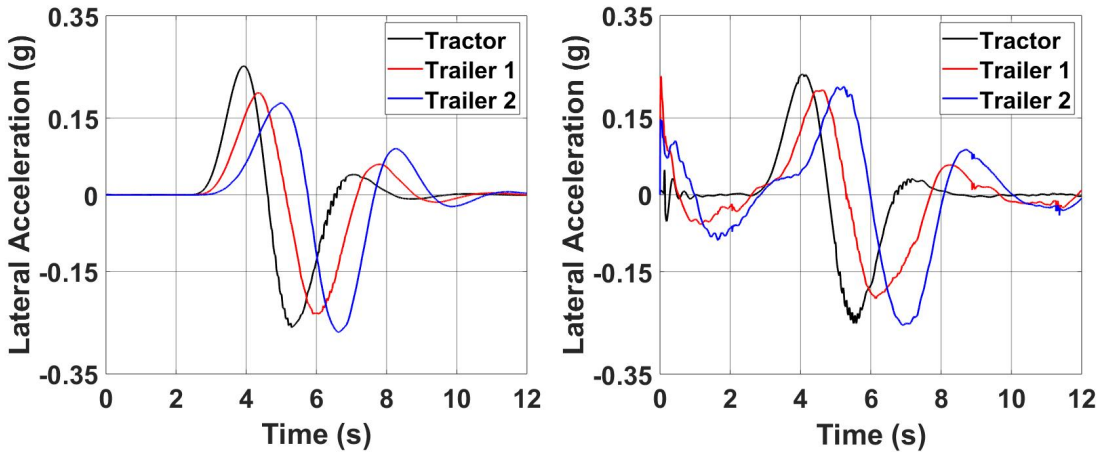

(a) (b)

FIGURE A.28: Time history of lateral accelerations for the B-train double derived from (a) the numerical simulations, and (b) HIL real-time simulations.

Table 4.4 - Case No. 3

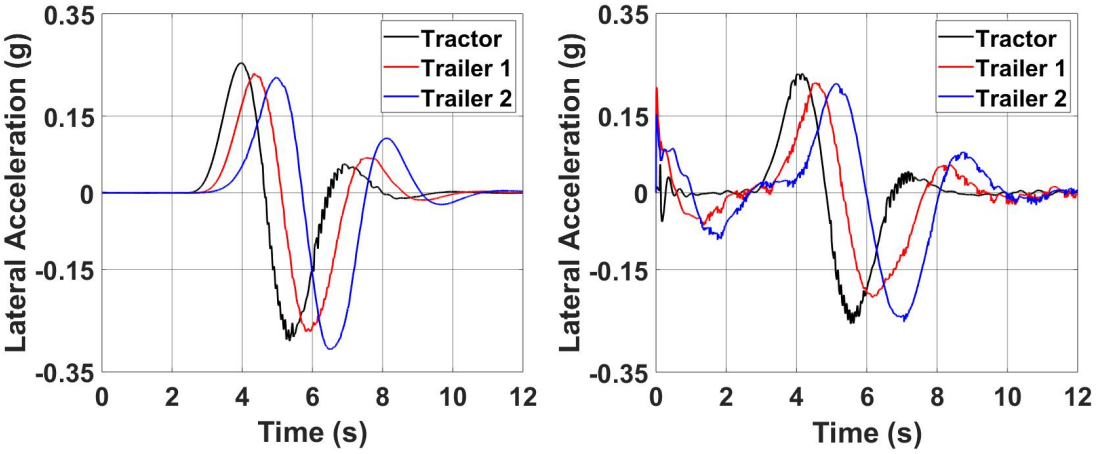

(a) (b)

FIGURE A.29: Time history of lateral accelerations for the B-train double derived from (a) the numerical simulations, and (b) HIL real-time simulations.

Table 4.4 - Case No. 4

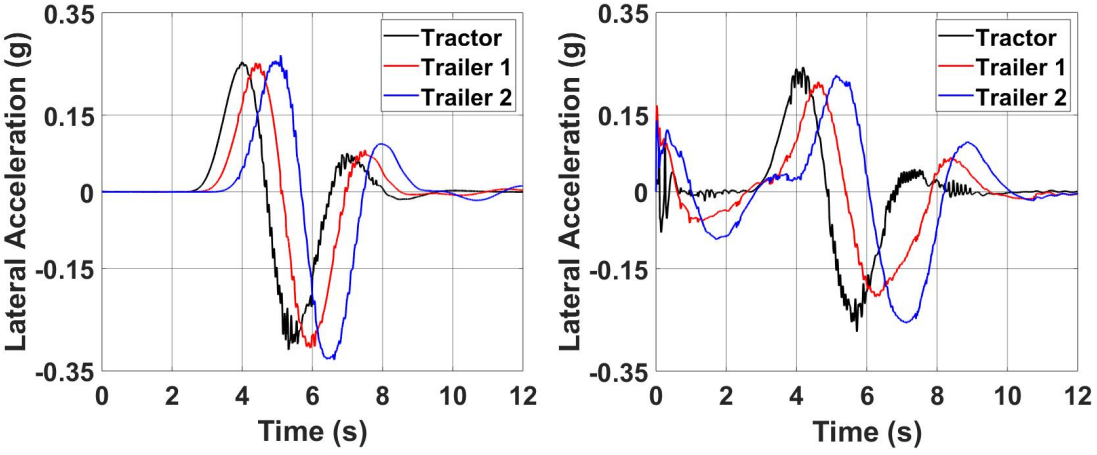

(a) (b)

FIGURE A.30: Time history of lateral accelerations for the B-train double derived from (a) the numerical simulations, and (b) HIL real-time simulations.